รายงานวิจัยฉบับสมบูรณ์

โครงการ
การประยุกต์ใช้การวิเคราะห์ภาพในการตรวจสอบการเสียรูปแบบไม่สม่ำเสมอของวัสดุอาหารประเภทหดตัวได้ในระหว่างการอบแห้ง

โดย

ดร.มธุรดา จิโนรส

พฤษภาคม พ.ศ. 2561

สัญญาเลขที่ TRG5880109

รายงานวิจัยฉบับสมบูรณ์

โครงการ
การประยุกต์ใช้การวิเคราะห์ภาพในการตรวจสอบ การเสียรูปแบบไม่สม่ำเสมอของวัสดุอาหาร ประเภทหดตัวได้ในระหว่างการอบแห้ง

ดร.มธุรดา จิโนรส
ภาควิชาวิศวกรรมอาหาร คณะวิศวกรรมศาสตร์
สถาบันเทคโนโลยีพระจอมเกล้าเจ้าคุณทหารลาดกระบัง

สนับสนุนโดยสำนักงานกองทุนสนับสนุนการวิจัยและต้นสังกัด

Executive Summary

Deformation is a phenomenon that is common during drying. Generally, deformation is evaluated and reported in terms of volumetric shrinkage. However, volumetric shrinkage cannot be used to describe non-uniform deformation, which commonly takes place during drying of shrinkable materials such as biopolymers, fruits and vegetables. In this study, algorithms and software were developed to first reconstruct 3D images from 2D images, and then to monitor and characterize non-uniform deformation of such images. Agar gel with different sugar contents were used as the test materials and were allowed to undergo drying at different rates.

The developed image reconstruction algorithms were successfully validated with standard geometrical shapes. Various image-based parameters, both in two dimensions, I.e., projected area, perimeter, major axis length, minor axis length, equivalent diameter, aspect ratio, extents, fractal dimension and various shape parameters; and in three dimensions, i.e., volume, surface area, various sphericities, Wadell's roundness, radius ratio and Hoffmann shape entropy, were then calculated. The results showed that extent and fractal dimension could be used to identify the onset and to monitor non-uniform deformation in two dimensions, while sphericity could be used for such tasks in three dimensions.

However, choosing appropriate parameters is very important if non-uniform deformation is to be monitored; widely used parameters cannot always be used for such a purpose. For example, extent, fractal dimension and sphericity could be used to identify the onset and to monitor non-uniform deformation for a cube but these parameters could not be used to monitor a real food deforms non-uniformly in three dimensions with rugged surface such as puffed banana slices. This is most probably because 2D top-view images are not adequate for the evaluation of a sample with rugged surface. In this case, for the 2D-based parameters, aspect ratio and the other extent (calculated from the ratio of projected area to Feret's diameters) could be used to indicate the start of the non-uniform deformation period; Wadell's sphericity represented the 3D-based parameters that could be used to perform the similar task. These parameters, however, could not be used to monitor the volume change of the samples. 3D-based volume and surface area along with the Wadell's sphericity should instead be used to monitor the puffing of banana slices.

The relationship between the drying conditions as well as composition and non-uniform deformation behavior and its subsequent influence on physical and physicochemical properties of the model food materials based on the developed image-based parameters was investigated. The obtained information should be useful for future development of a real-time and/or in situ monitoring and control system for a drying process of high-value foods and soft biomaterials via the use of a computer vision system (CVS).

Acknowledgements

The Investigator expresses her sincere appreciation to the Thailand Research Fund (TRF) and King Mongkut's Institute of Technology Ladkrabang for supporting the study financially through the New Researcher Grant no. TRG 5880109.

Abstract

Project Code: TRG5880109

Project Title: Use of Image Analysis as a Tool to Understand Non-Uniform Deformation Behavior of Food Materials during Drying

Investigator: Dr. Maturada Jinorose

E-mail Address: maturada.ji@kmitl.ac.th

Project Period: 2 years

Deformation is a phenomenon that is common during drying. Generally, deformation is evaluated and reported in terms of volumetric shrinkage; however, volumetric shrinkage cannot be used to describe non-uniform deformation, which commonly takes place during drying of various food materials, including fruits and soft confectionary such as soft candy, gel, gelatin and jelly products. Although attempts have recently been made to describe non-uniform deformation via the use of different image-based indicators, most of these indicators can only describe deformation in only one or two dimensions; the results are also mostly qualitative in nature. In this study, algorithms and software were developed to characterize the three-dimensional changes of shape, size and appearances of model food materials, agar gel with different sugar contents, undergoing drying at different rates. Appropriate parameters, that can be used to monitor non-uniform deformation of the materials were calculated and tested. The developed image reconstruction algorithms, which reconstruct 3D images from 2D images, were successfully validated with standard geometrical shapes. Various image-based parameters, both in two dimensions, i.e., projected area, perimeter, major axis length, minor axis length, equivalent diameter, Feret's diameter, extents, aspect ratio, form factor, fractal dimension and various shape parameters; and in three dimensions, i.e., image-based volume, surface area, various sphericities, Wadell's roundness, radius ratio and Hoffmann shape entropy, were then calculated and tested for their suitability to monitor such a deformation. The results showed that choosing appropriate parameters is very important if non-uniform deformation is to be monitored; widely used parameters

cannot always be used for such a purpose. For example, extent and fractal dimension could be used to identify the onset and to monitor non-uniform deformation in two dimensions, while sphericity could be used for such tasks in three dimensions for a cube but these parameters could not be used to monitor a slice deforms non-uniformly in three dimensions with rugged surface. Relationships between composition and physical as well as physicochemical properties of foods and their deformation were investigated to understand how non-uniform deformation behavior (and its subsequent influence on physical and physicochemical properties) was affected by the combined effect of composition and drying rate. The obtained information should be useful for future development of a real-time and/or in situ monitoring and control system for a drying process of high-value foods and soft biomaterials via the use of a computer vision system (CVS).

Keywords: Apparent Characteristics; Shape; Deformation; Image Analysis; Quality Evaluation; Drying

บทคัดย่อ

รหัสโครงการ : TRG5880109

ชื่อโครงการ : การประยุกต์ใช้การวิเคราะห์ภาพในการตรวจสอบการเสียรูปแบบไม่สม่ำเสมอของวัสดุอาหารประเภทหดตัวได้ในระหว่างการอบแห้ง

ชื่อนักวิจัย : ดร.มธุรดา จิโนรส
สถาบันเทคโนโลยีพระจอมเกล้าเจ้าคุณทหารลาดกระบัง

E-mail Address : maturada.ji@kmitl.ac.th

ระยะเวลาโครงการ : 2 ปี

การเปลี่ยนรูปเป็นปรากฏการณ์หนึ่งที่พบได้ทั่วไปในระหว่างการอบแห้ง โดยทั่วไปการเปลี่ยนรูปจะถูกประเมินและรายงานในรูปของการหดตัวเชิงปริมาตร อย่างไรก็ตามการหดตัวเชิงปริมาตรไม่สามารถใช้บอกการเปลี่ยนรูปแบบไม่เป็นเอกรูป ซึ่งมักเกิดขึ้นในระหว่างการอบแห้งวัสดุประเภทหดตัวได้ เช่น พอลิเมอร์ชีวภาพ ผักและผลไม้ ได้ มีความพยายามอธิบายการเปลี่ยนรูปแบบไม่เป็นเอกรูปโดยใช้ตัวบ่งชี้จากภาพ ทว่าตัวบ่งชี้เหล่านี้มักอธิบายการเปลี่ยนรูปได้เพียงในเชิงหนึ่งหรือสองมิติ ผลที่ได้จึงมักอยู่ในรูปข้อมูลเชิงคุณภาพ ในงานวิจัยนี้ขั้นตอนวิธีและซอฟต์แวร์ได้ถูกพัฒนาขึ้น เพื่อวิเคราะห์ลักษณะการเปลี่ยนแปลงเชิงสามมิติของรูปร่าง, ขนาด และลักษณะปรากฏ ของตัวอย่างอาหาร วุ้น agar ซึ่งมีปริมาณน้ำตาลแตกต่างกันถูกใช้เป็นวัสดุในการทดสอบและถูกอบแห้งด้วยอัตราเร็วที่แตกต่างกัน คำนวณและทดสอบตัวแปรที่เหมาะสมในการเฝ้าสังเกตการเปลี่ยนรูปแบบไม่เป็นเอกรูป ขั้นตอนวิธีการสร้างภาพขึ้นใหม่ที่พัฒนาขึ้นเพื่อสร้างภาพสามมิติจากการประกอบภาพสองมิติถูกตรวจสอบความแม่นยำกับวัสดุรูปทรงเรขาคณิตพื้นฐาน พารามิเตอร์เชิงภาพต่าง ๆ ทั้งในเชิงสองมิติ ได้แก่ พื้นที่แบบฉาย, เส้นรอบรูป, ความยาวแกนเอกและแกนโท, เส้นผ่านศูนย์กลางสมมูล, ขอบเขต (Extents), มิติสาทิสรูป และพารามิเตอร์รูปร่างต่าง ๆ และเชิงสามมิติ ได้แก่ ปริมาตร, พื้นที่ผิว, ภาวะทรงกลมแบบต่าง ๆ, ความกลม, อัตราส่วนรัศมี และเอนโทรปีรูปร่างของ Hoffmann (Hoffmann shape entropy) ได้ถูกคำนวณและทดสอบ จากการศึกษาพบว่าการเลือกพารามิเตอร์ที่เหมาะสมในการสังเกตนั้นสำคัญมาก โดยเฉพาะในกรณีการเสียรูปแบบไม่เป็นเอกรูป พารามิเตอร์ที่เป็นที่นิยมใช้โดยทั่วไปใช่ว่าจะเหมาะสมกับงานเสมอไป เช่น ขอบเขตและมิติสาทิสรูปสามารถใช้ใช้เฝ้าสังเกตและระบุการเริ่มต้นเปลี่ยนรูปของรูปร่างทรงลูกบาศก์ในเชิงสองมิติ ขณะที่ภาวะทรงกลมสามารถใช้ได้ในเชิงสามมิติ ทว่าพารามิเตอร์เหล่านี้กลับไม่

สามารถใช้ได้ในกรณีวัสดุแผ่นกลมที่เปลี่ยนรูปทั้งสามมิติและมีผิวขรุขระ เช่น กล้วยแผ่นอบกรอบ ความสัมพันธ์ระหว่างสมบัติทางกายภาพ เคมีกายภาพของอาหาร กับการเปลี่ยนรูปได้ถูกทำการศึกษาเพื่อให้เข้าใจถึงพฤติกรรมการเปลี่ยนรูป (และอิทธิพลของการเปลี่ยนรูปต่อสมบัติทางกายภาพและเคมีกายภาพ) ซึ่งได้รับผลจากองค์ประกอบและอัตราการทำแห้ง ข้อมูลที่ได้รับนี้สามารถนำมาพัฒนาระบบเฝ้าสังเกตและควบคุมกระบวนการแบบทันทีสำหรับการอบแห้งอาหารมูลค่าสูงและวัสดุชีวภาพเนื้อนิ่มด้วยระบบคอมพิวเตอร์วิทัศน์

คำหลัก : ลักษณะปรากฏ; รูปร่าง; การเปลี่ยนรูป; การวิเคราะห์ภาพ; การประเมินคุณภาพ; การอบแห้ง

Contents

1. Introduction

During drying of foods and soft biomaterials, moisture migrates from inner structure through the porous structure to the environment. Moisture gradients, which result from the differences in the moisture level at different positions within the structure, lead to non-uniform deformation of the materials, especially those composed of soluble protein and/or polysaccharides such as fruits and soft confectionary, e.g., soft candy, gel, gelatin and jelly products. It is well recognized that foods with different compositions and structures behave differently during drying and that important physical transformations, e.g., casehardening, distortion and changes of shape, are affected by the combined effect of drying conditions and food composition. However, without detailed quantitative information on the deformation behavior, this combined effect cannot be effectively established. Unfortunately, deformation, which is in most cases non-uniform in nature, is very difficult to evaluate.

Normally, deformation is reported in terms of volumetric shrinkage, which is calculated from the volume of a product at any instant and its initial volume. However, volumetric shrinkage cannot be used to describe non-uniform deformation as this parameter only considers the change of the overall volume of a material. It was indeed reported that while the shape of a material might have significantly changed, the volumetric shrinkage might not. This deficiency deserves significant attention as drying does not cause only the change of volume but also the change of the shape of a material. This change of shape significantly affects heat/mass transfer area and hence the drying behavior, which in turn results in altered time-temperature history of the material. Since physical, physicochemical and nutritional properties of a dried product are expectedly affected by its time-temperature history, it is of great importance that deformation be described and expressed adequately. Very limited studies are nevertheless available on describing food deformation behavior, especially when non-uniform deformation is involved. This is because it is not easy to quantify (and not only qualify) the change of shape. Although deformation is clearly non-uniform, it is difficult to assign any value to quantify the degree of non-uniformity, especially when describing the non-uniformity in three dimensions is of interest.

Based on the aforementioned arguments, it is interesting to investigate the use of image analysis as a tool to understand the non-uniform deformation behavior of foods during drying as affected by both the drying conditions and food composition. In this study, agar gel with different solids contents and compositions were used as a model

material. This model material is selected as it should allow the determination of the effect of food composition, in combination with the drying conditions, in a controllable manner. Sugar is known to significantly affect deformation since it might cause casehardening, leading to surface rigidity and other forms of distortion and shape changes, which are of interest as well.

Algorithms and software were developed to characterize the changes of the model foods during drying at different rates. Various dimension, shape and deformation parameters were investigated; appropriate parameters that can quantitatively represent the non-uniform deformation characteristics of the model foods were calculated and tested; validation of such parameters was also made on real food materials (i.e., carrot cubes and banana slices).

The developed image reconstruction algorithms were successfully validated with standard geometrical shapes. The results showed that choosing appropriate parameters is very important if non-uniform deformation is to be monitored; widely used parameters cannot always be used for such a purpose. The extent, fractal dimension and sphericity could be used to identify the onset and to monitor non-uniform deformation of model food materials. However, in case of a real food deforms non-uniformly in three dimensions with rugged surface such as puffed banana slices, aspect ratio and the other extent (calculated from the ratio of projected area to Feret's diameter) could be used to indicate the start of the non-uniform deformation period; Wadell's sphericity represented the 3D-based parameters that could be used to perform the similar task. These parameters, however, could not be used to monitor the volume change of the samples. 3D-based volume and surface area along with the Wadell's sphericity should instead be used to monitor the materials deforms non-uniformly in three dimensions with rugged surface.

The relationship between the drying conditions as well as composition and non-uniform deformation behavior and its subsequent influence on physical and physicochemical properties of the model food materials based on the developed image-based parameters were also investigated. The obtained information should be useful for future development of a real-time and/or in situ monitoring and control system for a drying process of high-value foods and soft biomaterials via the use of a computer vision system (CVS).

2. Materials and Methods

Please refer to the Appendix for detailed Materials and Methods used in the study.

3. Results and Discussion

Please refer to the Appendix for detailed Results and Discussion of the study.

4. Conclusions

Please refer to the Appendix for detailed Conclusions of the study.

Outputs of the Project

I. Refereed papers in international journals (1 papers)

1. Jinorose, M., Stienkijumpai, A., Devahastin, S., 2017, "Use of Digital Image Analysis as a Monitoring Tool for Non-uniform Deformation of Shrinkable Materials during Drying," Journal of Chemical Engineering of Japan, 50(10), pp. 785-791. (2016 IF = 0.629)

II. Papers presented at international conferences (3 papers)

1. Stienkijumpai, A., Jinorose, M., Devahastin, S., 2018, "Development and use of three-dimensional image analysis algorithms to evaluate puffing of banana slices undergone combined hot air and microwave drying," *Proceedings of the 21st International Drying Symposium (IDS 2018)*, September 11-14, 2018, Valencia, Spain.
2. Jinorose, M., Sukkapat, N., Tangnobnom, B., Onsumlee, P., Thongnuch, P., Devahastin, S., 2016, "Use of Non-Static Drying Procedures to Reduce Non-Uniform Deformation of a Solid Food and Its Monitoring via Image-Based Parameters," *Proceedings of the 9th Thai Society of Agricultural Engineering International Conference (TSAE 2016)*, September 8-10, 2016, Bangkok, Thailand.
3. Stienkijumpai, A., Jinorose, M., Devahastin, S., 2016, "Quantification of Non-uniform Deformation of Shrinkable Materials during Drying via Digital Image Analysis," *Proceedings of the 20th International Drying Symposium (IDS 2016)*, August 7-10, 2016, Gifu, Japan.

III. Research Networks

Collaborations have been made with King Mongkut's University of Technology Thonburi (Prof. Dr. Sakamon Devahastin, Department of Food Engineering).

IV. Awards Received

The Investigator has received the Best Research Award – In recognition of excellence in drying research from the 20th International Drying Symposium (IDS 2016), August 7-10, 2016, Gifu, Japan.

Appendix

VOL. 50
NO. 10
OCTOBER
2017

JCEJ
JOURNAL OF
CHEMICAL ENGINEERING
OF JAPAN

SCEJ The Society of Chemical Engineers, Japan

The Society of Chemical Engineers, Japan

JCEJAQ 50(10)
755-806(2017)
ISSN 0021-9592

Journal of Chemical Engineering of Japan, Vol. 50, No. 10, pp. 785–791, 2017 **Research Paper**

Use of Digital Image Analysis as a Monitoring Tool for Non-Uniform Deformation of Shrinkable Materials during Drying

Maturada JINOROSE[1], Anyanun STIENKIJUMPAI[1] and Sakamon DEVAHASTIN[2]

[1] *Department of Food Engineering, Faculty of Engineering, King Mongkut's Institute of Technology Ladkrabang, 1 Soi Chalongkrung 1, Ladkrabang, Bangkok 10520, Thailand*

[2] *Advanced Food Processing Research Laboratory, Department of Food Engineering, Faculty of Engineering, King Mongkut's University of Technology Thonburi, 126 Pracha u-tid Road, Tungkru, Bangkok 10140, Thailand*

Keywords: Biomaterial, Fractal Dimension, Shape Factor, Sugar, Shrinkage

Deformation is a phenomenon that is common during drying. Generally, deformation is evaluated and reported in terms of volumetric shrinkage. However, volumetric shrinkage cannot be used to describe non-uniform deformation, which commonly takes place during drying of shrinkable materials such as biopolymers, fruits and vegetables. In the present study, algorithms and software were developed to first reconstruct 3D images from 2D images, and then to monitor non-uniform deformation of such images. Agar gel with different sugar contents were used as the test materials and were allowed to undergo drying at different rates. The developed image reconstruction algorithms were successfully validated with standard geometrical shapes. Various image-based parameters, both in two dimensions, i.e. projected area, perimeter, major axis length, minor axis length, equivalent diameter, extent and fractal dimension; and in three dimensions, i.e. volume, sphericity, Wadell's sphericity, Wadell's roundness, radius ratio and Hoffmann shape entropy, were then calculated. The results showed that extent and fractal dimension could be used to identify the onset and to monitor non-uniform deformation in two dimensions, while sphericity could be used for such tasks in three dimensions.

Introduction

Drying is a process that removes volatile substances (mostly water) from a material and turns it into a solid product (Mujumdar, 2015). During drying, changes, including physical, chemical and microstructural changes, occur. Among these changes, deformation (i.e. change of shape and/or size) is one of the most common (Niamnuy *et al.*, 2008). Generally, deformation is quantified by direct measurement using such instruments as a Vernier caliper (Raghavan and Silveira, 2001) or evaluated and reported in terms of the volumetric shrinkage, which can be calculated from the ratio of the material volume at any instant to the initial volume; such simple methods as the solid or liquid displacement method can be employed to determine the volumetric shrinkage (Sansiribhan *et al.*, 2010).

Despite its simplicity and widespread use in drying-related studies, volumetric shrinkage cannot be used to describe non-uniform deformation, which commonly takes place during drying of highly shrinkable materials such as biopolymers and even fruits and vegetables (Panyawong and Devahastin, 2007). In fact, it has been reported that, while two pieces of a material undergoing two different drying methods may suffer much different patterns of deformation (or in other words, different changes of shape and/or size), their volumetric shrinkage values may still be similar (Devahastin *et al.*, 2004; Devahastin and Niamnuy, 2010). Since the change of shape significantly affects heat and mass transfer, which in turn affects physical, physicochemical, microstructural and nutritional properties of a dried product, it is important that non-uniform deformation be adequately described and monitored.

To achieve the aforementioned objective, image analysis has been applied to describe deformation. Various shape factors have been proposed for such a purpose. Nevertheless, most of the reported works were performed using shape factors that can only describe deformation in only one or two dimensions, although deformation usually occurs in all three directions; the results are also mostly qualitative in nature (Niamnuy *et al.*, 2014). This is due to the fact that acquisition of two-dimensional (2D) images is much easier than that of three-dimensional (3D) images. It is important to note, however, that 2D image-based analysis can never accurately represent non-uniform deformation.

Recently, limited attempts have been made to describe shape using indicators derived from 3D image-based information. For example, Bullard and Garboczi (2013) reported

Received on January 27, 2017; accepted on June 16, 2017
DOI: 10.1252/jcej.17we035
Presented at the 20th International Drying Symposium (IDS 2016), Gifu, August 2016
Correspondence concerning this article should be addressed to M. Jinorose (E-mail address: maturada.ji@kmitl.ac.th).

that any properties such as volume, dimension and sphericity of 3D-shaped particles (star-shape) could be calculated from a mathematical model developed from macroscopic parameters and surface integrals. Various sphericity-based shape factors, i.e. true roundness, sphericity, radius ratio of bounding spheres, Hofmann shape entropy, Wadell's roundness and Wadell's sphericity, were indeed calculated from the particle surface integrals. It was found that the roundness could capture the particle shape better than the other tested shape factors. Radvilaite *et al.* (2016) who attempted to characterize various grain shapes, i.e. chickpea, maize and bean, also found that a mathematical model developed from spherical harmonics (SH) could be used to classify the shape rather well. It must be noted nevertheless that the shape identification or characterization has usually been done only on standard or drawn-shapes; real materials with complex shapes have not been tested due to the limitation of an image acquisition algorithms.

Although there currently exists several options for software such as Autodesk Recap 360 (Autodesk Inc.), Agisoft Photoscan (Agisoft, LLC) or Visual SFM (http://ccwu.me/vsfm/) that can be used to construct 3D images from 2D images, ready-made reconstructed 3D images are in most cases incomplete and must be further adjusted and calibrated if accurate information including shape, volume and surface are to be obtained and, in particular, quantified. Since deformation occurs in all dimensions, using 3D image-based analysis should accurately represent non-uniform deformation better than a simpler 2D image-based method.

In the present study, algorithms and software were developed to first reconstruct 3D images from 2D images; standard geometrical shapes were used for the validation and calibration purposes. Various parameters, both in two dimensions, i.e. projected area, perimeter, major axis length, minor axis length, equivalent diameter, fractal dimension and extent; and in three dimensions, i.e. volume, sphericity, Wadell's sphericity, Wadell's roundness, radius ratio and Hoffmann shape entropy, were then calculated and compared to determine if they have the capability of monitoring non-uniform deformation. Agar gel with different sugar contents were used as the test materials and allowed to undergo drying at different rates.

1. Experimental

1.1 Agar gel preparation

Two percent (w/w) granulated purified agar (Product no. 1016141000, Merck Millipore Corp.) was mixed with sugar (at 0, 10 or 20% w/w) and added to distilled water. The mixture was stirred at room temperature at 100 rpm for 1 h, and then heated to 95°C; stirring continued at 150 rpm for 10 min. The mixture was then allowed to cool for 10 min, after which it was poured into a silicone mold to form agar cubes with the dimensions of 1.9×1.9×1.9 cm. The cubes were taken out of the mold after 1 h setting at room temperature (25±2°C). The initial moisture content of agar gel with 0% sugar was 45.1±0.5% (d.b.), while those of the gels with 10% and 20% sugar were 5.5±0.2% (d.b.) and 2.7±0.1% (d.b.), respectively.

1.2 Drying experiments

Drying experiments were conducted in a convective hot air dryer (UM500, Memmert GmbH+Co. KG) at two different drying temperatures (60 and 80°C). The drying air velocity was maintain at ≈0.1 m/s. Three cubes were taken at each predetermined drying time (every 1 h until moisture content was lower than 0.1% (d.b.)). The cubes were weighed and their images taken. The volume of the cubes was also determined.

1.3 Moisture content determination

Sample was weighed using a 4-digit digital balance with an accuracy of ±0.0002 g (BSA224S-CW, Sartorius Lab Instruments GmbH & Co. KG), and then dried in a hot air oven (UM500, Memmert GmbH+Co. KG) at 105±2°C until constant mass was obtained as per the AOAC method 984.25 (2000). The moisture content (M.C.) of the sample was then calculated as Eq. (1):

$$\text{M.C. (\% d.b.)} = \frac{m_i - m_{bd}}{m_{bd}} \times 100 \tag{1}$$

Here, m_i and m_{bd} are the mass of the sample at any instant and bone-dry mass of the sample, respectively.

1.4 Volume determination

Volume of a sample was determined using a liquid displacement method with 25 mL Hubbard–Carmick specific gravity bottle (1620–25, Corning Inc.) and 95% *n*-heptane (AR 1078, RCI Labscan Ltd.) (density ≈0.680 g cm^{-3}) as the working liquid (Sansiribhan *et al.*, 2010). The volume of the sample was calculated as Eq. (2).

$$V_l = \frac{m - m_s}{\rho} \tag{2}$$

Here, m, m_s and ρ are the mass of the sample in the air, mass of the sample in the solvent and density of the solvent, respectively.

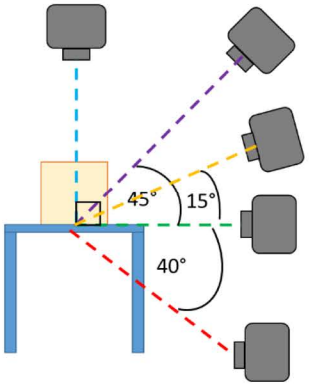

Fig. 1 Image acquisition positions

1.5 Image acquisition

2D images of a sample were first captured by a CMOS-sensor digital camera (G16, Canon Inc.) within a light box with the dimensions of 40×40×40 cm. The employed lighting system consists of 4 fluorescent lamps (Daylight FL8WT5, Lamptan Lighting Technology Co., Ltd.) placed around the top of the box. Images were taken from five angles as shown in **Figure 1**. The sample was placed on a 360° rotating platform, which rotated at 3 rpm (18 s per round). Images were taken at 1 s intervals (or at every 20° rotation).

3D images were reconstructed from the 2D images using Autodesk Recap 360 software (Autodesk Inc.). A post-processing step was performed to reduce unwanted objects using MeshLab (ISTI-CNR, Visual computing Lab., http://www.meshlab.net).

1.6 Image analysis

In the case of 2D image analysis, the first analysis step involved foreign object elimination from the acquired image, which was done via MATLAB Release 2016b (The MathWorks, Inc.). Each image was cropped to 512×512 pixels (without distortion of shape). Image segmentation was then performed by converting an RGB image into a binary image using Otsu's thresholding method (Jinorose *et al.*, 2014). Edge detection and hole filling were subsequently performed to extract an area of interest. Various parameters, i.e. projected area, perimeter, major axis length, minor axis length, equivalent diameter, extent (a ratio of project area to bounding box area) and fractal dimension, which was calculated using the box counting method, were then extracted from the area of interest. All parameters were calculated using algorithms written in MATLAB® and equations of Neal and Russ (2012).

In the case of 3D image analysis, after a 3D image was reconstructed, the image was converted into an STL file and imported into COMSOL Multiphysics® version 3.5 (COMSOL, Inc.) to calculate the volume and various shape factors, i.e. sphericity, Wadell's sphericity, Wadell's roundness, radius ratio and Hoffmann shape entropy, using Eqs. (3) to (7). These parameters were selected due to their simplicity. It was also reported that sphericity could be used to well describe the shape of an object in three dimensions (Bullard and Garboczi, 2013). Fine mesh setting was adopted when assigning meshes to the image prior to the volume determination.

$$\text{Sphericity} = \frac{(36\pi)^{1/6} V^{1/3}}{SA^{1/2}} \tag{3}$$

$$\text{Wadell's sphericity} = \frac{SA_V}{SA} \tag{4}$$

$$\text{Wadell's roundness} = \frac{\sum_{i=1}^{N} R_i}{NR_{max}} \tag{5}$$

$$\text{Radius ratio} = \frac{R_{min}}{R_{max}} \tag{6}$$

$$\text{Hoffmann shape entrop} = \frac{1}{\ln\left(\frac{1}{3}\right)} \sum_{i=1}^{3} p_i \ln p_i \tag{7}$$

1.7 Validation of reconstructed images

The accuracy of the image reconstruction algorithms was verified by applying such algorithms to selected standard shapes, i.e. cube, cylinder, cone and sphere (with dimensions varied from 1 to 2.5 cm as shown in **Table 1**).

Comparison of the obtained image-based results was made with the results obtained from the conventional methods, i.e. use of Eqs. (8) to (11) to calculate the volume and liquid displacement method. Various dimensions that were needed for Eqs. (8) to (11) were obtained via direct measurement using a Venier caliper (Mitutoyo, Japan) with an accuracy of ±0.002 mm. Information pertaining to a 3D image (i.e. volume), which was reconstructed from the developed algorithms, was also compared with that obtained from conventional 3D measurement techniques, i.e., laser scanning via a commercial scanner (Artec 3D, Artec Eva, Luxembourg).

$$\text{Cube} \qquad V_c = D_1 \times D_2 \times D_3 \tag{8}$$

$$\text{Cylinder} \qquad V_c = \pi \left(\frac{D}{2}\right)^2 h \tag{9}$$

$$\text{Cone} \qquad V_c = \frac{\pi}{3} \left(\frac{D}{2}\right)^2 h \tag{10}$$

$$\text{Sphere} \qquad V_c = \frac{4}{3}\pi \left(\frac{D}{2}\right)^3 \tag{11}$$

Here, V_c is the volume and D is the average diameter. D_1, D_2 *and* D_3 are the diameters in x-axis, y-axis and z-axis, respectively, and h is the average height.

All experiments and analyses were performed at least in duplicate.

Table 1 Size and dimensions of standard shapes as measured using a Vernier calliper

Shape	Dimension [mm]
Cube	10.30±0.05
	15.32±0.04
	20.06±0.20
	25.21±0.07
	30.21±0.08
Cylinder	D=10.20±0.00, H=10.23±0.02
	D=15.28±0.03, H=15.26±0.03
	D=20.25±0.03, H=20.40±0.02
Cone	D=10.11±0.02, H=10.19±0.01
	D=15.08±0.02, H=15.00±0.00
	D=20.25±0.08, H=20.33±0.03
Sphere	D=9.55±0.03
	D=16.31±0.06
	D=19.74±0.03

Note: D = diameter and H = height

2. Results and Discussion

2.1 Validation of reconstructed 3D images

3D images were reconstructed from 2D images as exemplified in **Figure 2**. It was found that the developed algorithms yielded satisfactory results in terms of volume (**Table 2**). The differences between the results obtained from the image reconstruction algorithms and those from the calculation and measurements were usually lower than 10%, except in the case of very small samples (smaller than 1.5 cm). This is because of the capture limit of the developed algorithms; the algorithms could best be used to determine the size of an object that is larger than 1.5 cm and smaller than 2 cm in any dimension. It is important to note that the tested commercial laser scanner could not be accurately used to determine the size of an object that is smaller than 1.0 cm in any dimension as well.

As shown in Table 2, liquid displacement and calculation methods exhibited standard deviations among replicates of each sample of less than 5% regardless of the size or dimension of the sample. On the other hand, the developed algorithms exhibited deviations of less than 10% in most cases, except when a sample was too small (i.e. in the cases of 1×1×1-cm cube and 1-cm height cone) or pointed-shape cone. No standard deviations are reported in the case of laser scanning measurement as only one replicate was made.

Resulted obtained from the laser scanner, calculation and developed algorithms compared with liquid displacement (which considered the traditional or standard method) usually had less than 5% difference except for small samples (smaller than 1.5 cm) regardless of the shapes. Therefore, it could be concluded the deviation between method of measurement was related with size (not too small, especially smaller than 1 cm).

2.2 Effect of drying temperature

Drying experiments were conducted at two different drying temperatures, i.e. 60°C (slow drying) and 80°C (moderate drying), at an air velocity around 0.1 m/s to study the effect of drying rate on the test material deformation; selected images of the samples at different drying time are shown in **Figure 3**. Only agar gel with 0% sugar was tested in this case. Initially, the sample deformed rather uniformly. However, upon prolonged drying, the sample started to deform non-uniformly. The point (time) where non-uniform deformation started to take place depended on the rate of drying; higher drying air temperature resulted in earlier non-uniform deformation. Nevertheless, if the results were considered based on the moisture content, the rate of dry-

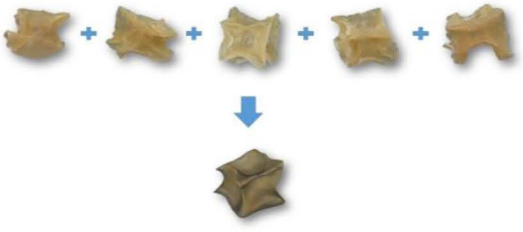

Fig. 2 Sample reconstructed 3D images

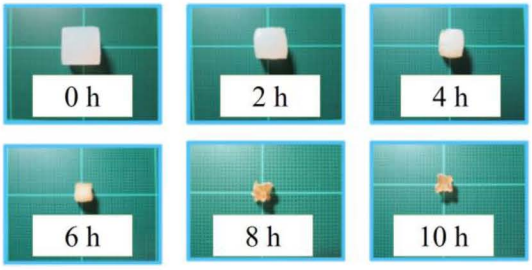

Fig. 3 Deformation of agar gel (0% sugar) during drying at 80°C

Table 2 Comparison between the volume obtained from image reconstruction, calculation and measurement

Shape	Volume [mm³]						
	Liquid displacement	Laser scanner		Calculation		Developed algorithms	
	Value	Value	%Diff	Value	%Diff	Value	%Diff
Cube	1060.855±3.926 (0.370%)	998.50	5.878	1091.293±6.457 (0.592%)	2.869	1373.726±214.154 (15.589%)	29.492
	3523.325±23.662 (0.672%)	3550.00	0.757	3595.639±16.264 (0.452%)	2.052	3684.058±191.206 (5.190%)	4.562
	8227.685±335.320* (4.076%)	8096.00	1.601	8069.858±50.530 (0.626%)	1.918	8330.946±143.877 (1.727%)	1.255
	15506.783±297.389* (1.918%)	15530.00	0.150	16015.294±55.319 (0.345%)	3.281	15398.571±203.819 (1.324%)	0.698
	25837.384±401.700** (1.555%)	27110.00	4.925	27561.607±54.813 (0.199%)	6.673	N/A	N/A
Cylinder	809.613±15.009 (1.854%)	787.20	2.768	835.650±1.887 (0.226%)	3.216	781.156±34.675 (4.439%)	3.515
	2744.375±22.322 (0.813%)	2560.00	6.718	2798.299±16.780 (0.600%)	1.965	2523.203±230.335 (9.129%)	8.059
	6441.789±77.726 (1.207%)	6075.00	5.694	6572.247±18.725 (0.285%)	2.025	6400.149±141.118 (2.161%)	0.646
Cone	287.346±18.312 (6.373%)	322.10	12.095	272.766±1.124 (0.412%)	5.074	238.815±12.174 (5.098%)	16.889
	965.897±7.710 (0.798%)	978.50	1.305	893.024±2.369 (0.265%)	7.545	969.849±64.733 (6.675%)	0.409
	2291.348±13.786 (0.602%)	2270.00	0.932	2182.90.6±19.575 (0.897%)	4.733	2367.782±192.138 (8.115%)	3.336
Sphere	425.826±8.261 (1.940%)	454.90	6.828	456.533±4.375 (0.958%)	7.211	327.866±103.092 (31.443%)	23.005
	2240.407±29.785 (1.329%)	2234.00	0.286	2273.200±24.184 (1.064%)	1.464	2041.038±224.519 (11.000%)	8.899
	3958.053±88.282 (2.230%)	3988.00	0.757	4027.567±21.225 (0.527%)	1.756	4029.170±445.117 (11.047%)	1.797

Note: Percent differences were calculated in comparison with the liquid displacement values. Laser scanning analysis was performed only in single replication.

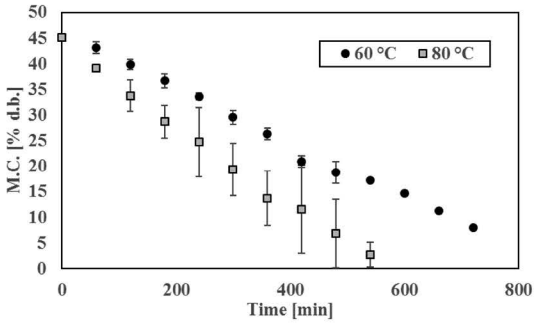

Fig. 4 Drying curves of agar gel (0% sugar) at different drying temperatures

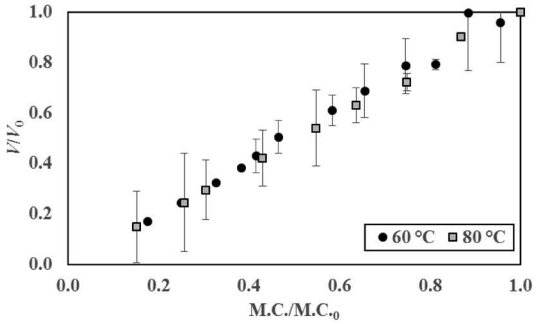

Fig. 5 Volume ratio as a function of moisture ratio of agar gel (0% sugar). 0 = initial value

ing did not have any significant effect on the point (moisture content) where non-uniform deformation started to take place.

Higher drying air temperature expectedly led to a higher drying rate as shown in **Figure 4**. Volume changes of the samples undergoing drying at both temperatures were not different if considered at the same moisture ratios as shown in **Figure 5**. At a moisture ratio of lower than 0.4, non-uniform deformation started to take place; the results agreed well with those observed visually.

2.3 Image-based information

Before the effect of sugar content was assessed, it is interesting to first determine if and which image-based parameters can be used to describe non-uniform deformation. Both 2D and 3D parameters were calculated.

Figure 6 shows the 2D image-based parameter evolutions as a function of the moisture ratio. When considering which parameters could be used to describe non-uniform deformation (or in other words, change of shape), only the fractal dimension and extent could be used. It is seen that these two parameters did not significantly vary until the moisture ratio was around 0.4, beyond which their values started to decline. Fractal dimension and extent decreased by less than 10% from their initial values as the moisture ratio decreased from unity to the value of around 0.4. This is in contrast to the significant drop in the values of other parameters; projected area, for example, decreased by around 50%.

This corresponded to the point where non-uniform deformation was visually observed to start. Other parameters, on the other hand, decreased right from the start of the drying process. For this reason, if the non-uniform deformation is to be monitored, only fractal dimension or extent should be used. On the other hand, if only volumetric shrinkage is to be monitored, any other parameters could also be used.

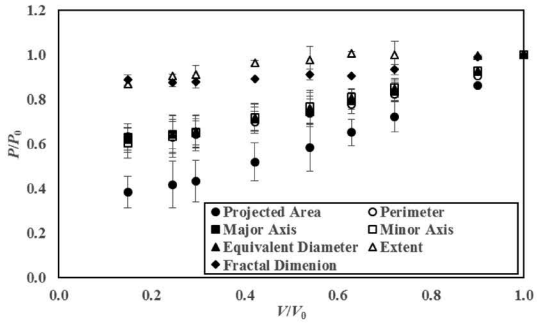

Fig. 6 2D parameter evolutions as a function of moisture ratio of agar gel (0% sugar) during drying at 80°C; P = parameter of interest; 0 = initial value

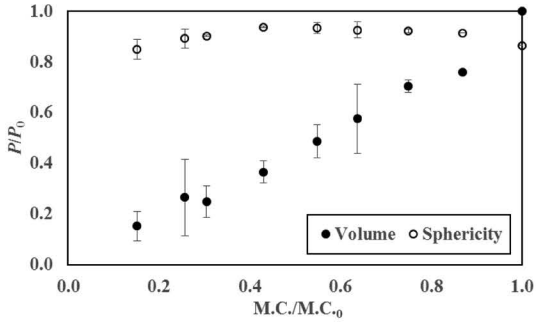

Fig. 7 3D parameter evolutions as a function of moisture ratio of agar gel (0% sugar) during drying at 80°C; P = parameter of interest; 0 = initial value

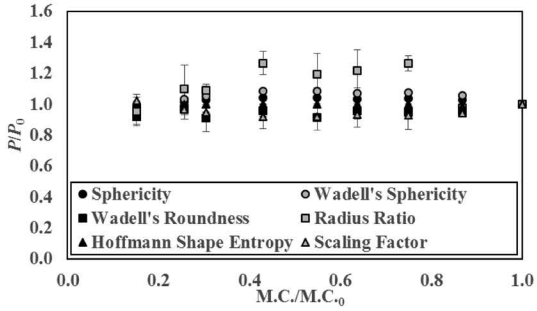

Fig. 8 Sphericity evolutions as a function of moisture ratio of agar gel (0% sugar) during drying at 80°C

Figure 7 shows the 3D image-based parameter evolutions as a function of the moisture ratio. The volume values were those of the reconstructed 3D images. Only sphericity exhibited a similar trend to those of the fractal dimension and extent, and hence should be used to monitor the non-uniform deformation. Nevertheless, if the volumetric shrinkage is to be monitored, volume could also be used. Note that the

volume of the reconstructed 3D images was in all cases no more than 10% different from the values obtained via the liquid displacement method. Therefore, the reconstruction process could be said to be quite successful.

Since sphericity was noted to be capable of monitoring non-uniform deformation, various sphericity factors were further studied, i.e. Wadell's sphericity, Wadell's roundness, Hoffmann shape entropy and radius ratio; the results are shown in **Figure 8**. It is seen that the general trends of the results belonging to the different sphericity factors were similar. The simple sphericity value should then be regarded as the most suitable parameter for non-deformation evaluation due to its simplicity.

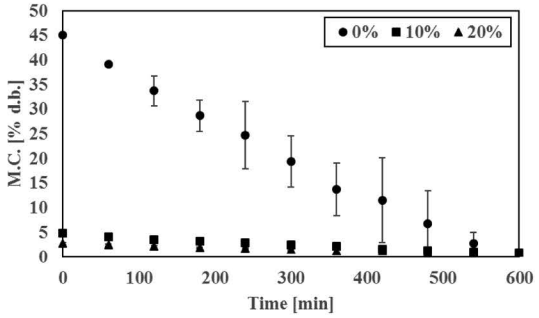

Fig. 9 Drying curves of agar gel with different sugar contents during drying at 80°C

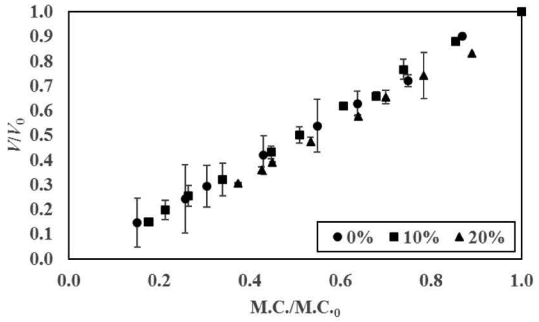

Fig. 10 Volume ratio as a function of moisture ratio of agar gel with different sugar contents during drying at 80°C

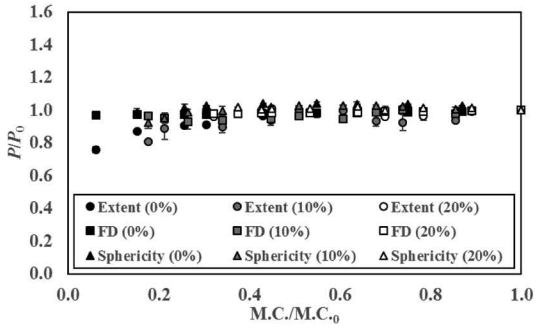

Fig. 11 Deformation parameter evolutions as a function of moisture ratio of agar gel with different sugar contents during drying at 80°C

2.4 Effect of sugar content

After determining suitable image-based parameters for the description of non-uniform deformation, selected parameters including fractal dimension, extent and sphericity were applied to study the effect of sugar (solid) content on the deformation characteristics of agar gel.

Drying of the gel with a higher sugar content was slower, as expected. **Figure 9** shows the drying curves of agar gel containing different sugar contents at 80°C. Although the initial moisture contents of agar gel with 10% and 20% sugar were greatly different from that of the gel with 0% sugar, the evolutions of the volumetric shrinkage of the gel with different sugar contents as a function of the moisture ratio were similar (**Figure 10**). For this reason, volumetric shrinkage can be used to monitor the degree of shrinkage, but cannot used to indicate the onset of non-uniform deformation.

Similar observations (as mentioned earlier) were noted when considering the results of other image-based parameters (**Figure 11**). The results showed that at moisture ratios lower than 0.4, non-uniform deformation started to take place. Extent and fractal dimension could be used to identify the onset and to monitor non-uniform deformation in two dimensions, while sphericity could be used for such tasks in three dimensions, regardless of the sugar content.

In the case of the gel sample with a sugar content of 20% (or an initial moisture content of 2.7%), non-uniform deformation was not observed from the data presented in Figure 11. This is probably because the solids content of such a sample was high, resulting in a more dense structure that could resist deformation. Drying also took place much more slowly, and hence led to the lower level of moisture gradients that could in turn result in the non-uniform deformation. This combined effect most probably led to the absence of the non-uniform deformation in this case.

Conclusions

Algorithms were developed to characterize and quantify non-uniform deformation of model food materials. Various parameters, both in two dimensions and three dimensions, were calculated. Sugar content and drying temperature did not pose any significant effect on the deformation if the samples were assessed at the same moisture ratios. Extent and fractal dimension could describe the deformation characteristics in two dimensions, while sphericity could be used to describe deformation in three dimensions. The developed algorithms should be useful for future development of a monitoring and control system for a drying process of high-value foods and soft biomaterials.

Acknowledgements

The authors express their sincere appreciation to the Thailand Research Fund (TRF) for supporting the study financially through its New Researcher Grant awarded to Author Jinorose (Grant No. TRG 5880109) and Senior Research Scholar Grant awarded to Author Devahastin (Grant No. RTA 5880009).

Nomenclature

D	=	diameter of the circle or sphere	[mm]
D_1, D_2, D_3	=	length of each side of sample	[mm]
h	=	height from base to crown point	[mm]
m	=	mass of sample in air	[g]
m_{bd}	=	bone-dry mass of the sample	[g]
m_i	=	mass of sample at any instant	[g]
m_s	=	mass of sample in liquid	[g]
N	=	number of radius of 3D image	
p_1	=	ratio between length of each dimension to sum of length of all dimension in 3D image	
R_i	=	radius from the center to surface of 3D image sample	[voxel]
R_{max}	=	radius of the smallest circumscribe sphere in 3D image	[voxel]
R_{min}	=	radius of the biggest inscribe sphere in 3D image	[voxel]
SA	=	surface area of sample from 3D image	[mm^2]
SA_V	=	surface area of sphere that have same volume from 3D image	[mm^2]
V	=	volume of sample from 3D image	[mm^3]
V_l	=	volume of sample from liquid displacement method	[mm^3]
ρ	=	Density of solvent	[g cm^{-3}]

Literature Cited

Bullard, J. W. and E. J. Garboczi; "Defining Shape Measures for 3D Star-Shaped Particles: Sphericity, Roundness, and Dimensions," *Powder Technol.*, **249**, 241–252 (2013)

Devahastin, S., P. Suvamakuta, S. Soponronnarit and A. S. Mujumdar; "A Comparative Study of Low-Pressure Superheated Steam and Vacuum Drying of a Heat Sensitive Material," *Dry. Technol.*, **22**, 1845–1867 (2004)

Devahastin, S. and C. Niamnuy; "Modelling Quality Changes of Fruits and Vegetables during Drying: A Review," *Int. J. Food Sci. Technol.*, **45**, 1755–1767 (2010)

Jinorose, M., S. Prachayawarakorn and S. Soponronnarit; "A Novel Image-Analysis Based Approach to Evaluate Some Physicochemical and Cooking Properties of Rice Kernels," *J. Food Eng.*, **124**, 184–190 (2014)

Mujumdar, A. S.; "Principles, Classification, and Selection of Dryers," Handbook of Industrial Drying, 4th ed., A. S. Mujumdar ed., pp. 3–29, CRC Press, Boca Raton, U.S.A. (2015)

Neal, F. B. and C. J. Russ; Measuring Shapes, pp. 231–290, CRC Press, Boca Raton, U.S.A. (2012)

Niamnuy, C., S. Devahastin, S. Soponronnarit and G. S. V. Raghavan; "Modeling Coupled Transport Phenomena and Mechanical Deformation of Shrimp during Drying in a Jet Spouted Bed Dryer," *Chem. Eng. Sci.*, **63**, 5503–5512 (2008)

Niamnuy, C., S. Devahastin and S. Soponronnarit; "Some Recent Advances in Microstructural Modification and Monitoring of Foods during Drying: A Review," *J. Food Eng.*, **123**, 148–156 (2014)

Panyawong, S. and S. Devahastin; "Determination of Deformation of a Food Product Undergoing Different Drying Methods and Conditions via Evolution of a Shape Factor," *J. Food Eng.*, **78**, 151–161 (2007)

Radvilaitė, U., A. Ramirez-Gómez and R. Kačianauskas; "Determining the Shape of Agricultural Materials Using Spherical Harmonics," *Comput. Electron. Agric.*, **128**, 160–171 (2016)

Raghavan, G. S. V. and A. M. Silveira; "Shrinkage Characteristics of Strawberries Osmotically Dehydrated in Combination with Microwave Drying," *Dry. Technol.*, **19**, 405–414 (2001)

Sansiribhan, S., S. Devahastin and S. Soponronnarit; "Quantitative Evaluation of Microstructural Changes and Their Relations with Some Physical Characteristics of Food during Drying," *J. Food Sci.*, **75**, E453–E461 (2010)

The 20th International Drying Symposium (IDS 2016)
Gifu, JAPAN, 7-10 August 2016

D-6-5

QUANTIFICATION OF NON-UNIFORM DEFORMATION OF SHRINKABLE MATERIALS DURING DRYING VIA DIGITAL IMAGE ANALYSIS

Anyanun STIENKIJUMPAI[1], Maturada JINOROSE[1*] and Sakamon DEVAHASTIN[2]

[1]Department of Food Engineering, Faculty of Engineering, King Mongkut's Institute of Technology Ladkrabang
1 Soi Chalongkrung 1, Ladkrabang, Bangkok 10520, Thailand
Tel.:+66-02-329-8356, E-mail: maturada.ji@kmitl.ac.th

[2]Department of Food Engineering, Faculty of Engineering, King Mongkut's University of Technology Thonburi
126 Pracha u-tid Road., Bangmod, Bangkok 10140, Thailand
sakamon.dev@kmutt.ac.th

Abstract: Deformation is a phenomenon that is common during drying. Generally, deformation is evaluated and reported in terms of volumetric shrinkage. However, volumetric shrinkage cannot be used to describe non-uniform deformation, which commonly takes place during drying of shrinkable materials such as biopolymers, fruits and vegetables. In this study, algorithms and software were developed to characterize the deformation of model food materials (i.e., agar gel with different sugar contents) undergoing drying at different rates. Various parameters, both in two dimensions, i.e., projected area, perimeter, major axis length, minor axis length, equivalent diameter, extent and fractal dimension; and in three dimensions, i.e., volume and surface area as well as sphericity, were calculated. Appropriate parameters that can quantitatively represent the non-uniform deformation of the materials were extent, fractal dimension and sphericity; sphericity could be used to describe deformation in three dimensions, while extent and fractal dimension could describe the deformation characteristics in two dimensions.

Keywords: fractal dimension, image reconstruction, shape factor, sugar content, volumetric shrinkage

INTRODUCTION

Drying is a process that removes volatile substances (mostly water) from a material and turns it into a solid product (Mujumdar, 2006). During drying changes including physical, chemical and microstructural changes occur. Among these changes, deformation (i.e., change of shape and/or size) is one of the most common. Generally, deformation is evaluated and reported in terms of the volumetric shrinkage, which can be calculated from the ratio of the material volume at any instant to the initial volume; such simple methods as liquid displacement method can be employed to determine the volumetric shrinkage. However, volumetric shrinkage cannot be used to describe non-uniform deformation, which commonly takes place during drying of highly shrinkable materials such as biopolymers and even fruits and vegetables (Panyawong and Devahastin, 2007). In fact, it has been reported that while two pieces of a material undergoing two different drying methods might suffer much different patterns of deformation (or, in other words, different changes of shape and/or size), their volumetric shrinkage values might still be similar (Devahastin et al., 2004; Devahastin and Niamnuy, 2010). Since the change of shape significantly affects heat and mass transfer, which in turn affects physical and physicochemical properties of a dried product, it is important that deformation must be adequately described and expressed.

Recently, attempts have been made to describe deformation using indicators derived from image-based information. For example, Igathinathane et al. (2008) reported that other than rectangularity, extent (ratio of projected area to size of a rectangular bounding box) could also be used as an indicator to describe the change of a rectangular shape. Jinorose et al. (2014) also found that fractal dimension of a captured image could be used as an indicator of shape change for rice kernels. Nevertheless, most of these indicators can only describe deformation in only one

or two dimensions; the results are also mostly qualitative in nature.

Nowadays, three-dimensional image acquisition is no longer limited only to a large-scale production environment. Reconstruction techniques have been developed that allow user to reproduce a 3-dimensional model from two-dimensional images using such software as Autodesk Recap 360 (Autodesk Inc., San Rafael, CA), Agisoft Photoscan (Agisoft, LLC, St. Petersburg, Russia) or Visual SFM (http://ccwu.me/vsfm/). It should be noted that these reconstruction techniques can also be used to acquire 3D parameters, including volume, overall surface area and various shape parameters, which can then be used as deformation descriptors of the reconstructed model. Nevertheless, ready-made reconstructed 3D model is in most cases incomplete and must be further adjusted and calibrated if accurate information is to be obtained and, in particular, quantified.

In this study, algorithms and software were developed to quantify the deformation of model food materials (agar gel with different sugar contents). Various parameters, both in two dimensions, i.e., projected area, perimeter, major axis length, minor axis length, equivalent diameter, fractal dimension and extent; and in three dimensions, i.e., volume and surface area as well as sphericity, were calculated.

MATERIALS AND METHODS

Agar gel preparation

In this study, granulated purified agar (Product no. 1016141000, Merck Millipore, Germany) was used. Agar at 2% (w/w) was mixed with sugar (at 0 or 20% w/w) and added to distilled water. The mixture was stirred at 100 rpm for 1 h and then heated to 95 °C and stirred at 150 rpm for 10 min. The mixture was allowed to cool for 10 min. The mixture was then poured into a silicone mold to form agar cubes with the dimensions of 1.9 ×1.9 ×1.9 cm; the cubes were taken out of the mold after 1 h setting at 25 °C.

Drying experiments

Drying experiments were conducted in a convective hot air dryer (Memmert, UM55, Germany) at two different drying temperatures (60 and 80 °C).

Image acquisition

Two-dimensional images of a sample were captured by CMOS-sensor digital camera (Canon, G16, Japan) within a light box with the dimensions of 40×40×40 cm. The employed lighting system consists of 4 fluorescent lamps (Lamptan, F7, Thailand) placed around the top of the box. Images were taken from five angles as shown in Fig. 1. The sample was placed on a platform, which rotated at 4 rpm (15 s per round). Images were taken at every 1-s interval.

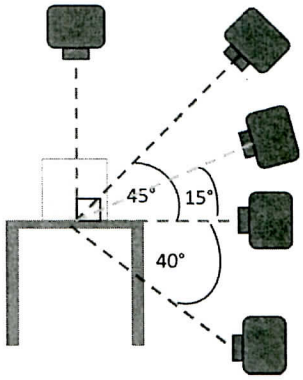

Fig. 1 Image acquisition positions

Three cubes were taken at each predetermined drying time to capture the images. Three-dimensional images were then reconstructed from the 2D images using Autodesk Recap 360 software.

Image analysis

For each 2D image, image pre-processing step was performed to reduce unwanted objects via MATLAB® (version R2014b, MathWork Inc., MA). Image segmentation was then performed by converting an RGB image into a binary image using Otsu's thresholding method. Edge detection and holes filling were then performed to extract area of interest. Various parameters were then extracted from the area of interest, i.e., projected area, perimeter, major axis length, minor axis length, equivalent diameter, extent and fractal dimension, which was calculated using the box counting method.

In the case of 3D image analysis, after a 3D model was generated by the software, the model image was converted into an STL file and imported into COMSOL Multiphysics® version 3.5 (COMSOL AB, Sweden) to calculate the sphericity (Neal and Russ, 2012), volume and surface area of the reconstructed object. 'fine mesh' setting was adopted when assigning meshes to the object prior to the calculation.

Moisture content determination

Fifteen g of a sample was weighed using a 4-digit digital balance (Yamato Electronic Balance, HB-120, Japan) and then dried in a hot air oven (Memmert, UM500, Germany) at 105±2 °C until constant mass was obtained as per AOAC method 984.25 (2000). The moisture content of the sample was then calculated as:

$$\text{Moisture content (\% d.b.)} = \frac{\mathrm{m}_i - m_{bd}}{m_{bd}} \times 100$$

where m_i, m_{bd} are the mass of the sample at any instant and bone-dry mass of the sample, respectively.

Volume determination

Volume of a sample was determined using a liquid displacement method with 99% n-heptane (density ≈ 0.6728 g cm^{-1}) as the working liquid.

RESULTS AND DISCUSSION

Effect of drying temperature

Drying experiments were conducted at two different drying temperatures, i.e., 60 °C (slow drying) and 80 °C (moderate drying), at an air velocity < 0.1 m/s to study the effect of the drying rate on the test material deformation; selected images of the sample at different drying time are shown in Fig. 2. Only the agar gel with 0% sugar was first tested. Initially, the sample deformed rather uniformly. However, upon prolonged drying, the sample started to deform non-uniformly. The point (time) where non-uniform deformation started to take place depended on the rate of drying; higher drying air temperature resulted in earlier non-uniform deformation. Nevertheless, if the results are considered based on the moisture content, the rate of drying did not have any significant effect on the point (moisture content) where non-uniform deformation started to take place.

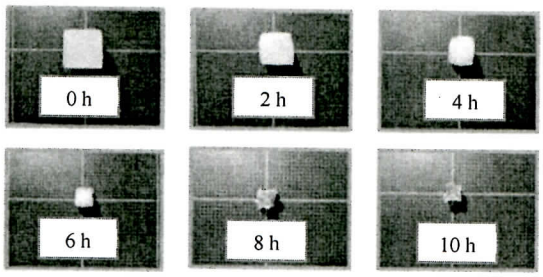

Fig. 2 Deformation of agar gel (0% sugar) during drying at 80 °C

Fig. 3 shows an example of a deformed reconstructed model of agar gel from 2D images.

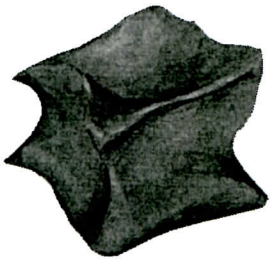

Fig. 3 Reconstructed image of agar gel

Higher drying air temperature expectedly led to a higher drying rate (Fig. 4). Volume changes (as assessed by liquid displacement method) of the samples undergoing drying at both temperatures were not different if considered at the same moisture ratios as shown in Fig. 5. At the moisture ratio of lower than 0.4, non-uniform deformation started to take place.

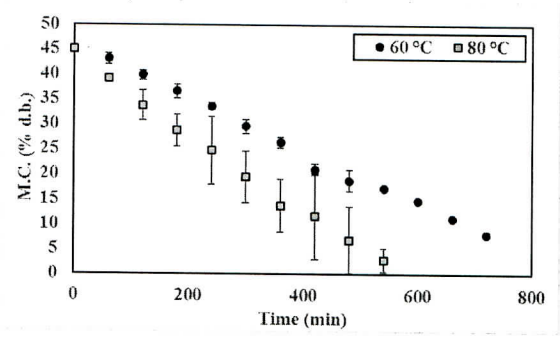

Fig. 4 Drying curves of agar gel (0% sugar) at different drying temperatures

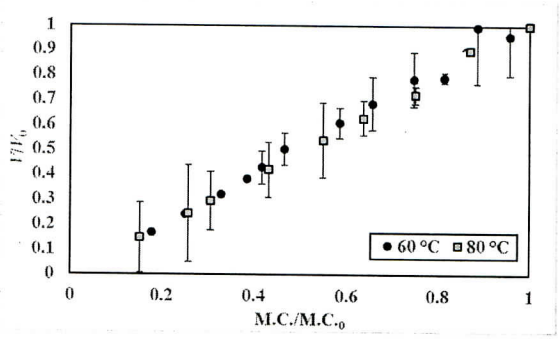

Fig. 5. Volume ratio as a function of moisture ratio of agar gel (0% sugar). 0 = initial value

Image-based information

Fig. 6 shows the 2D image-based parameter evolutions as a function of the moisture ratio. When considering which parameters could be used to describe the non-uniform deformation (or, in other words, change of shape), only the fractal dimension and extent could be used. It is seen that these two parameters did not significantly vary until the moisture ratio was around 0.4, beyond which their values started to decline. This corresponded to the point where non-uniform deformation was observed to start. Other parameters, on the other hand, decreased right from the start of the drying process. For this reason, if the non-uniform deformation is to be monitored, only fractal dimension or extent should be used. On the other hand, if only volumetric shrinkage is to be monitored, any other parameters should be used.

Fig. 7 shows the 3D image-based parameter evolutions as a function of the moisture ratio. The volume and surface area values were those of the reconstructed 3D models. Only the sphericity exhibited the similar trend to those of the fractal dimension and extent and hence should be used to monitor the non-uniform deformation. Again, if the volumetric shrinkage is to be monitored, volume and surface area should be used. Note that the calculated volume of the reconstructed 3D models was in any cases not more than 10% different from the values obtained via the liquid displacement method. Therefore, the reconstruction process could be said to be quite successful.

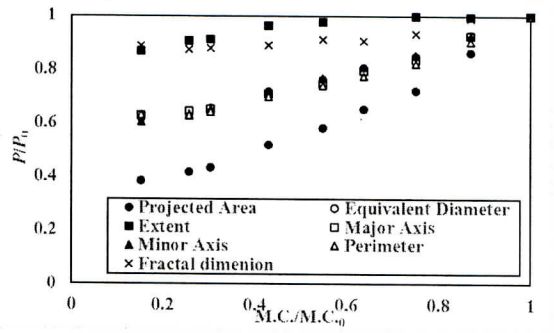

Fig. 6. 2D parameter ratio evolutions as a function of moisture ratio of agar gel (0% sugar) during drying at 80 °C. P = Parameter of interest; 0 = initial value

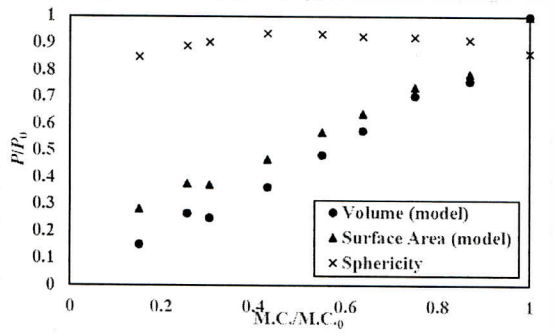

Fig. 7. 3D parameter ratio evolutions as a function of moisture ratio of agar gel (0% sugar) during drying at 80 °C. P = Parameter of interest; 0 = initial value

Effect of sugar content

Fig. 8 shows the drying curves of agar gels containing different solids (sugar) contents during drying at 80 °C. Drying of the gel with higher sugar content was very slow, as expected. The evolution of the volumetric shrinkage of the gels with different sugar contents as a function of the moisture ratio was nevertheless similar. Similar observations were noted for other image-based parameters.

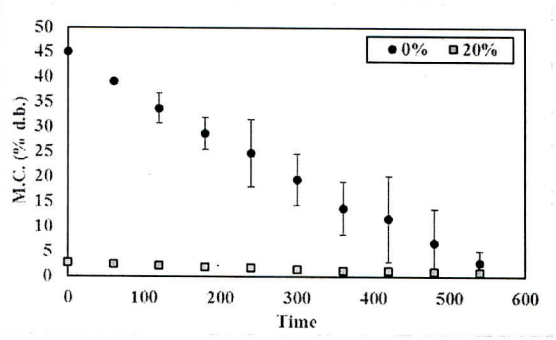

Fig. 8. Drying curves of agar gel with different sugar contents during drying at 80 °C

CONCLUSIONS

Algorithms were developed to characterize and quantify the non-uniform deformation of model food materials with different sugar contents undergoing drying at different rates. Various parameters, both in two dimensions and three dimensions were calculated. Sugar content and drying temperature in did not pose any significant effect on the deformation if the samples were assessed at the same moisture ratios. Extent and fractal dimension could describe the deformation characteristics in two dimensions, while sphericity could be used to describe deformation in three dimensions. The developed algorithms should be useful for future development of a monitoring and control system for a drying process of high-value foods and soft biomaterials.

ACKNOWLEDGEMENTS

The authors express their sincere appreciation to the Thailand Research Fund (TRF) for supporting the study financially through its New Researcher Grant awarded to Author Jinorose (Grant No. TRG5880109) and Senior Research Scholar Grant awarded to Author Devahastin (Grant No. RTA5880009).

REFERENCES

Aguilera, J.M; Stanley, D.W. Microstructural Principles of Food Processing and Engineering, 2nd edition, Aspen Publication, Gaithersburg, MD, 1999.

Devahastin, S.; Suvarnakata, P.; Soponronnarit, S.; Mujumdar, A.S. A comparative study of low-pressure superheated steam and vacuum drying of a heat sensitive material. Drying Technology 2004, 22(8), 1845-1867.

Devahastin, S.; Niamnuy, C.; Modelling quality changes of fruits and vegetables during drying: a review. International Journal of Food Science and Technology 2010, 45, 1755-1767.

Igathinathane, C.; Pordesimo, L.O.; Columbus, E.P.; Batchelor, W.D.; Methuku, S.R. Shape identification and particles size distribution from basic shape parameters using ImageJ. Computer and Electronics in Agriculture 2008, 63, 168-182.

Jinorose, M.; Prachayawarakorn, S.; Soponronnarit, S. A novel image-analysis based approach to evaluate some physicochemical and cooking properties of rice kernels. Journal of Food Engineering 2014, 124, 184-190.

Mujumdar, A.S. Principles, classification, and selection of dryers. In Handbook of Industrial Drying 3rd edition; Mujumdar, A.S., Ed.; CRC Press: Boca Raton, FL, 2006; 4-31.

Panyawong, S; Devahastin, S. Determination of deformation of a food product undergoing different drying methods and conditions via evolution of a shape factor. Journal of Food Engineering 2007, 78(1), 151-161.

Neal, F.B. and Russ, C.J. Measuring Shapes; CRC Press: Boca Raton, FL, 2012; 231-290.

PHF-25

Use of Non-Static Drying Procedures to Reduce Non-Uniform Deformation of a Solid Food and Its Monitoring via Image-Based Parameters

Maturada Jinorose[1]*, Nattawut Sukkapat[1], Benjaporn Tangnobnom[1], Pakorn Onsumlee[1], Pongsatorn Thongnuch[1], Sakamon Devahastin[2]

[1]*Department of Food Engineering, Faculty of Engineering, King Mongkut's Institute of Technology Ladkrabang, 1 Soi Chalongkrung 1, Ladkrabang, Bangkok 10520, Thailand.*
[2]*Advanced Food Processing Research Laboratory, Department of Food Engineering, Faculty of Engineering, King Mongkut's University of Technology Thonburi, 126 Pracha u-tid Road, Bangkok 10140, Thailand.*

Corresponding author: Maturada Jinorose. E-mail: maturada.ji@kmitl.ac.th

Abstract

Deformation is among the most important changes a solid food experiences during drying. This change usually results from the loss of moisture from the food matrix. As the rates of moisture loss at different locations within a sample are not equal, uniform deformation rarely takes place; a more extensive deformation indeed occurs at a position that experiences more rapid drying. To reduce non-uniform deformation, moisture gradient-induced stress must somehow be relaxed. Flipping or rotating a food sample during drying to allow all surfaces to experience similar time-averaged drying condition was proposed to help relax the stress and hence the non-uniform deformation. The capability of such techniques were investigated and the resulting deformation behavior was monitored through the use of selected image-based parameters, namely, normalized changes of the projected area and fractal dimension of the sample images as well as the rectangularity. Agar cubes were used as a test material and allowed to undergo hot air drying at 50°C. The results showed that flipping the cubes led to less non-uniform deformation. Normalized change of the fractal dimension was noted to be the most suitable parameter to describe non-uniform deformation of the agar cubes.

Keywords: Image analysis, Moisture gradients, Non-static drying, Agar, Shrinkage, Stress

1 Introduction

It is well recognized that food suffers both physical and chemical changes during drying, due mainly to the applied heat and moisture removal (Sokhansanj and Jayas, 2006). These changes are most of the time undesirable and may adversely affect the consumer acceptance of the products, especially when the changes involve such apparent characteristics of food as color, shape and size (Jinorose et al, 2009).

Deformation is among the most important changes a solid food experiences during drying. The change usually results from the loss of moisture from the food matrix. Deformation may be uniform if the rates of moisture loss at different locations within the matrix are equal. Unfortunately, uniform deformation rarely takes place as such rates are usually not equal (Aguilera and Stanley, 1999). A more extensive deformation occurs at a position that experiences more rapid drying. To reduce non-uniform deformation, moisture gradients and indeed moisture gradient-induced stress must somehow be relaxed. Flipping or rotating a food sample during drying to allow all surfaces to experience similar time-averaged drying condition may be an alternative to help relax the moisture gradients and thus reduce the non-uniform deformation. This reduction could be possible as a particular surface experiencing higher level of heat and hence higher rate of moisture removal is being refreshed after a drying interval has elapsed.

Since traditional methods that have been used to monitor deformation, including liquid displacement method, which results in the volumetric shrinkage data, cannot be effectively used to monitor non-uniform deformation, which does not involve only the change of volume but also change of shape (Devahastin et al.,

2004; Panyawong and Devahastin, 2007), an alternative evaluation or at least a monitoring method is required. Image analysis is a potential method for tackling such a limitation of the traditional evaluation and/or monitoring methods. It is necessary, however, to first determine which image-based parameters have an adequate capability to undertake the required task.

In this study, investigation of the capability of selected non-static drying procedures, namely, flipping and rotating a solid food sample, on moisture gradient (or moisture gradient-induced stress) relaxation and subsequent reduction of non-uniform deformation was performed. Selected image-based indicators were also tested to determine whether they can be used to monitor the non-uniform deformation behavior of a solid food sample undergoing different drying procedures.

2 Materials and Methods

2.1 Agar gel preparation

Agar (3 % w/w) was soaked in distilled water at room temperature (25°C ± 2°C) for 1 h. The mixture was heated using a water-bath at 95°C. After stirring the mixture in the water bath for 1 h, the mixture was poured into a silicone mold to form the cubes (1.9x 1.9x1.9 cm). The cubes were removed from the mold after 40 min; the cubes were kept at 4±1°C for 12 h prior to being used.

2.2 Drying experiments

A convective hot air tray dryer (Kluay Nam Thai Trading Group Co., Ltd., Bangkok, Thailand) was used for the drying experiments. Drying was conduced at a drying air temperature of 50°C and an air velocity of 1±0.1 m/s until the moisture content of a sample was lower than 20 % (d.b.).

Different modes of drying were assessed, namely, static drying as well as non-static drying where a sample was flipped or rotated during drying. In the case of non-static drying, flipping and rotation of a sample was made at every 30-min interval. In the case of flipping, a sample was flipped at every 30 min in the directions shown in Figure 1(a). In the case of rotation, a sample was rotated clockwise, as show in Figure 1(b), at every 30 min. Sampling was made at every 1 h to measure the moisture content as well as for image acquisition.

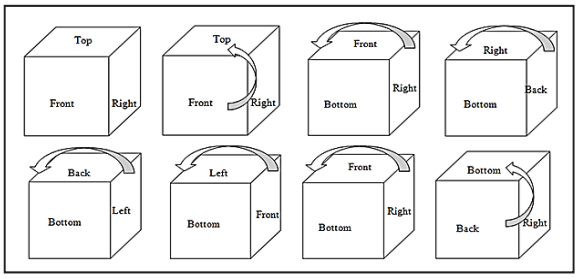

(a) Flipping directions

(b) Rotation directions

Figure 1 Flipping and rotation directions of a sample during non-static drying.

2.3 Image acquisition

Images were captured in a self-made image acquisition set-up (Figure 2) consisting of a 31x31x28-cm light box, 6500-K light source (Fluorescent lamp, Philips, TL-E Super 80, Thailand) and CCD digital camera (Samsung Digimax NV3, Korea), which was placed at the top of the box. A sample was placed on a platform, which is located 15 cm from the base of the box on a black background. Acquired images were transferred to a PC for further analysis by our own image acquisition algorithms.

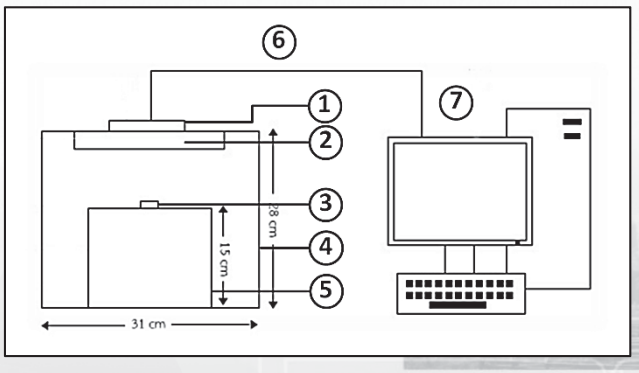

Figure 2 Image acquisition system. (1) CCD camera; (2) circular fluorescent lamp; (3) sample; (4) light box; (5) platform with black background; (6) USB cable; and (7) PC.

2.4 Image analysis

All image analysis algorithms were developed on MATLAB® 2012b (Mathworks, Inc., Natick, MA). Each image was first cropped to 700x700 pixel (without any change of the dimension and color depth). Segmentation was performed using Otsu's thresholding algorithm (Otsu, 1979) in combination with the 'greythresh' function of MATLAB to convert an RGB image to a binary image.

Projected area, perimeter, major axis, minor axis and equivalent diameter of a sample were extracted using 'regionprops' function. Fractal dimension of a sample image was calculated using the box counting method (Jinorose et al., 2014). Rectangularity (RTY) was calculated as described by Igathinathane et al. (2008) using the following equation:

$$\mathrm{RTY} = \frac{A_{\mathrm{ef}}}{H_{\mathrm{b}} \times W_{\mathrm{b}}};\ A_{ef} = \frac{\pi}{4}ab \quad (1)$$

where A_{ef} is the area of the smallest ellipse that can cover the rectangular object of interest (pixels), a is the major axis of the ellipse (pixels), b is the minor axis of the ellipse (pixels), H_b is the height of the bounding rectangle (pixels) and W_b is the width of the bounding rectangle (pixels).

2.5 Moisture content determination

A sample was dried in a hot air oven (Memmert, UM500, Germany) at 105±2°C until its mass was constant according to AOAC Method 984.25 (AOAC, 2000). Before and after drying, the sample was weighed using a 4-digit digital balance (Yamato Electronic Balance, HB-120, Japan). The moisture content of the sample was calculated from:

$$\text{Moisture content (\% d.b.)} = \frac{\mathrm{m}_i - m_{bd}}{m_{bd}} \times 100 \quad (2)$$

where m_i and m_{bd} are the masses of the sample before drying and after drying (bone-dry mass of the sample), respectively.

2.6 Volume determination

Volume of the sample was calculated using liquid displacement method with petroleum ether as the working liquid as per the method described by Sahin and Sumnu (2006). A beaker with petroleum ether was placed on a balance (Shimadzu, UX3200G, Japan). A sample was then submerged into the liquid. The sample volume was calculated as:

$$V = \frac{F}{\rho} \quad (3)$$

where V is the volume of the sample (cm^3), F is the buoyancy force (shown as weight change in g), ρ is density of working liquid.

3 Results and Discussion

3.1 Deformation description feasibility of image-based parameters

Prior to drying agar cubes suffered no deformation as shown in Figure 3(a). Upon drying, as expected, the cubes started to deform. After 8 h of drying at 50°C, the cubes suffered extensive deformation as can be seen in Figure 3(b); deformation was obviously non uniform and the cubes became very distorted.

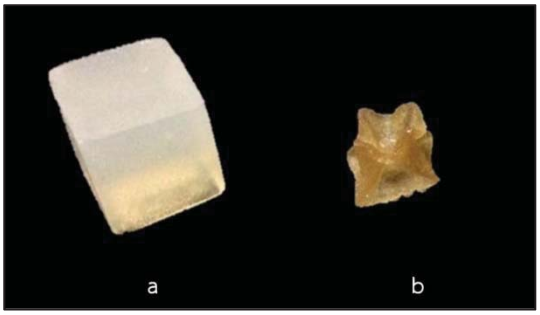

Figure 3 Deformation of agar cubes after drying for 8 h. (a) Before drying; (b) after drying

To determine which image-based parameters would be capable of monitoring non-uniform deformation, only the results of the static drying experiments were first assessed. The evolutions of the image-based parameters, namely, projected area, perimeter, major axis, minor axis, equivalent diameter, Feret's diameter, fractal dimension and rectangularity are shown in Figure 4. In the present case, agar cubes first suffered uniform deformation before it started to deform non-uniformly. This implies that if any image-based parameters are to be capable of monitoring the change of shape (which is more relevant to the non-uniform deformation) and not the change of size (which is more relevant to the uniform deformation),

such parameters should remain more or less unchanged during the initial non-uniform deformation period.

As can be seen in Figure 4, the normalized changes of all image-based parameters, except for fractal dimension and rectangularity, during the static drying experiments decreased until the X/X_0 had reached around 0.05 (which corresponds to the drying time of around 5 h as depicted in the drying curve (static drying case) shown in Figure 5. This means that only fractal dimension and rectangularity exhibit potential for monitoring the non-uniform deformation of agar cubes in our subsequent work. Note that the projected area, major and minor axes, perimeter and Feret's diameter are all the parameters that mainly describe the dimension and size; on the other hand, fractal dimension and rectangularity are the parameters that have been widely used to describe the shape (Igathinathane et al., 2008; Jinorose et al. 2014; Kerdpiboon et al., 2007; Stienkijumpai et al. 2016).

When the changes of the image-based parameters are plotted against the volumetric shrinkage as shown in Figure. 6, it is seen that the size-related parameters changed almost linearly with the shrinkage during the uniform deformation period, while the shape-related parameters remained almost unchanged. The shape-related parameters started to experience some changes only after the sample started to deform non-uniformly, which took place after drying for 5 h (corresponded to the $\Delta V/V_0$ value above 0.9 as seen in Figure 6

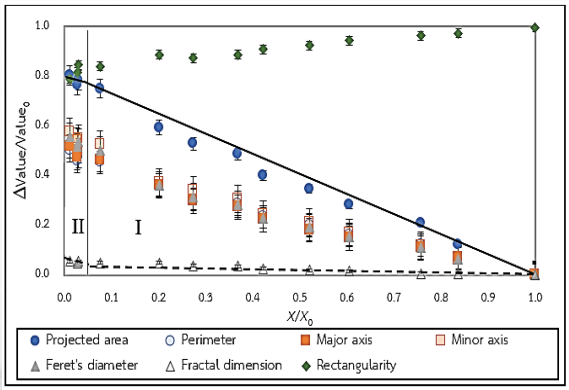

Figure 4 Normalized changes of image-based parameters as a function of moisture ratio of agar cubes during static drying. Value = Value of parameter of interest; 0 = initial value.

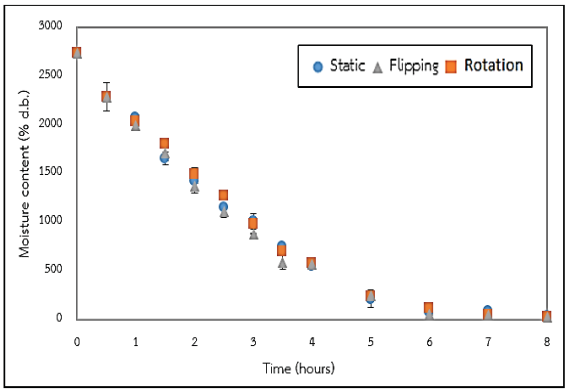

Figure 5 Drying curves of agar cubes undergoing different drying schemes.

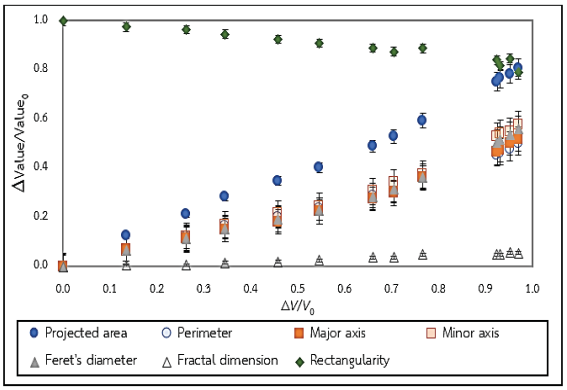

Figure 6 Normalized changes of image-based parameters as a function of volumetric shrinkage of agar cubes during static drying. *Value* = Value of parameter of interest; 0 = initial value *Value* = Value of parameter of interest; 0 = initial value.

3.2 Effect of non-static drying on deformation behavior of agar gel

During drying it was observed that the apparent characteristics of a sample as viewed from different sides were different. This is most probably because different sides of the sample were differently exposed to the drying air and hence exhibited different rates of moisture loss (and moisture gradient-induced stress), leading as a consequence to different patterns of deformation as can be seen in Figure 7. The effects of flipping and rotating a sample were determined and the results were compared with that obtained by static drying (i.e., drying with no sample flipping or rotation).

Figure 5 shows the drying curves of a sample undergoing drying of various schemes. During the first

5 h the moisture content rapidly decreased; afterwards, the moisture content decreased more slowly towards the equilibrium values. Flipping or rotating did not significantly result in accelerated drying. When considering the deformation of the sample, on the other hand, flipping resulted in the least deformation. The sample undergoing static drying suffered more deformation, as expected (see Figure. 7a and 7b). This is because flipping helped exposing all faces of the sample to heat in a more uniform fashion. Initially, a particular surface of the sample might have exposed to a higher level of heat; moisture removal from that sample surface would then be higher, leading to higher moisture gradient-induced stress. By flipping the sample, a surface with extensive exposure to the heat would be switched. The generated moisture gradient-induced stress would then be relaxed. As the stress was continuously relaxed throughout the whole drying process, less stress was accumulated and hence the lower level of deformation. It is surprising to note, however, that rotating the sample led to a higher level of deformation than static drying. This is because static drying involved no movement of the sample, leading to the sample adhering to the drying tray. Such an adherence resulted in the sample being able to withstand the change of shape as the bottom part of the sample stuck to the tray and retarded the change of the sample shape (Figure 7c).

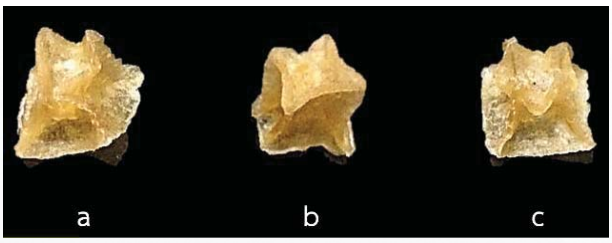

Figure 7 Deformation of agar cubes after drying at 50°C for 8 h. (a) Static drying; (b) drying with flipping and (c) drying with rotation.

When considering the normalized changes of the fractal dimension (Figure 8), it is seen that the changes of the fractal dimension of the different samples undergoing different drying schemes were quite dissimilar, especially during the latter part of the drying process. During an initial period of drying (moisture ratio of higher than around 0.5), the differences in the fractal dimension changes were not significant among the different samples; the rates of change were almost linear with the change of the moisture ratio. Beyond this initial period, however, the changes of the fractal dimension of the different samples started to be different. The sample undergoing flipping experienced a rather constant rate of change of the fractal dimension, while the samples undergoing static drying as well as rotation experienced non-constant rate of changes of the fractal dimension. The samples undergoing rotation suffered the most obvious change of the fractal dimension, which implies that such a sample suffered the most extensive non-uniform deformation. This illustrates that the normalized change of the fractal dimension could be used to monitor non-uniform deformation.

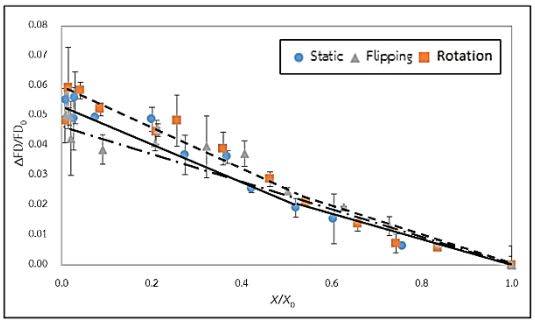

Figure 8 Normalized changes of fractal dimension as a function of moisture ratio of agar cubes undergoing different drying schemes at 50°C.

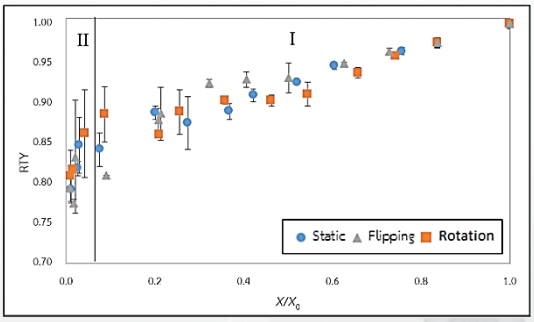

Figure 9 Normalized changes of rectangularity as a function of moisture ratio of agar cubes undergoing different drying schemes at 50°C.

Figure 9 shows the normalized changes of the rectangularity of the samples undergoing different drying schemes. The changes of the rectangularity could also be

used to monitor the non-uniform deformation but only when such a deformation was extensive, i.e., toward the end of the drying process. In addition, the changes of this parameter could not be used to well distinguish the different deformation patterns.

Just for comparison, the normalized changes of the projected area of the different samples are depicted in Fig. 10. It is seen that such a change could not be used to distinguish the different samples undergoing different drying schemes. This is because the different drying schemes did not differently affect the sample perimeter, which is the determining factor influencing the projected area. This phenomenon was noted despite the fact that the deformation patterns as observed visually were quite different. This implies that the projected area is not an adequate parameter to describe non-uniform deformation, which took place in the present case.

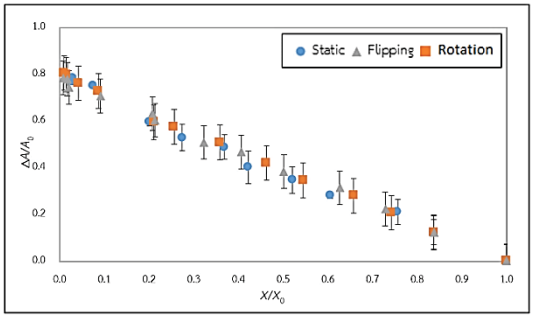

Figure 10 Normalized changes of projected area as a function of moisture ratio of agar cubes undergoing different drying schemes at 50°C.

4 Conclusions

In this study, attempts were made to identify appropriate image-based parameters that can be used to monitor non-unform deformation of a solid food (agar cubes). Three modes of drying, including static drying as well as drying with flipping and with rotation of a sample during the whole course of drying, were also assessed as a means to reduce non-uniform deformation. Normalized changes of fractal dimension of the sample images were noted to be able to monitor non-uniform deformation of the agar cubes. Flipping the cubes throughout the course of drying led to the samples with less non-uniform deformation.

5 Acknowledgements

The authors express their sincere appreciation to the Thailand Reserch Fund (TRF; Grant No. TRG 5880109) for supporting the study financially through its New Researcher Grant awarded to Author Jinorose.

6 References

Aguilera, J.M. and Stanley, D.W. 1999. Microstructural Principles of Food Processing and Engineering (2nd ed.). Gaithersburg, MD: Aspen Publication.

AOAC. 2000. Official Methods of Analysis (17th ed.). Gaithersburg. MD: Association of Official Analytical Chemists.

Devahastin, S., Suvarnakata, P., Soponronnarit, S., Mujumdar, A.S. 2004. A comparative study of low-pressure superheated steam and vacuum drying of a heat sensitive materials. Drying Technology 22(8), 1845-1867.

Igathinathane, C., Pordesimo, L.O., Columbus, E.P., Batchelor, W.D., Methuku, S.R. 2008. Shape identification and particles size distribution from basic shape parameters using ImageJ. Computer and Electronics in Agriculture 63, 168-182.

Jinorose, M., Devahastin, S., Blacher, S., Léonard, A. 2009. Apllication of image analysis in food drying. In: Ratti, C. (Ed.), Advances in Food Dehydration (pp. 63-95). Boca Rota: CRC Press.

Jinorose, M., Prachayawarakorn, S., Soponronnarit, S. 2014. A novel image-analysis based approach to evaluate some physicochemical and cooking properties of rice kernels. Journal of Food Engineering 124, 184-190.

Kerdpiboon, S., Devahastin, S., Kerr, W.L. 2007. Comparative fractal characterization of physical changes of different food products during drying. Journal of Food Engineering 83, 570-580.

Otsu, N. 1979. A thresholding selection method from gray-level. IEEE Transactions on System, Man and Cybernetics SMC-9. 62-66.

Panyawong, S., Devahastin, S. 2007. Determination of deformation of a food product undergoing different

drying methods and conditions via evolution of a shape factor. Journal of Food Engineering 78(1), 151-161.

Sahin, S., Sumnu, S.G. 2006. Physical Properties of Foods. New York: Springer Publishing.

Sokhansanj, S., Jayas, D.S. 2006. Drying of foodstuffs. In: Mujumdar, A.S. (Ed), Handbook of Industrial Drying (3rd ed.) (pp. 522–546). Boca Rota: CRC Press.

Stienkijumpai, A., Jinorose, M., Devahastin, S. 2016. Quantification of non-uniform deformation of shrinkable materials during drying via digital image analysis. In: Proceedings of the 20th International Drying Symposium (IDS 2016), D-6-5. 7-10 August 2016, Gifu, Japan.

IDS'2018 – 21st International Drying Symposium
València, Spain, 11-14 September 2018
DOI: http://dx.doi.org/10.4995/ids2018.2018.****

Development and use of three-dimensional image analysis algorithms to evaluate puffing of banana slices undergone combined hot air and microwave drying

Satienkijumpai, A.[a]; Jinorose, M.[a*]; Devahastin, S.[b]

[a] Department of Food Engineering. Faculty of Engineering. King Mongkut's Institute of Technology Ladkrabang, 1 Soi Chalongkrung 1, Ladkrabang, Bangkok, 10520, Thailand.

[b] Department of Food Engineering. King Mongkut's University of Technology Thonburi, 126 Pracha u-tid Road, Tungkru, Bangkok, 10140, Thailand.

*E-mail of the corresponding author: maturada.ji@kmitl.ac.th

Abstract

Puffing is an attractive alternative for the production of healthy crisp snacks without frying. Although image analysis has been used in some prior studies to evaluate puffing, such an evaluation was made only in one or two dimensions, which is inadequate when a sample deforms in three dimensions. In this study, use of combined hot-air and microwave drying to dry and puff banana slices was first evaluated. Algorithms were then developed to characterize the changes in the appearance of puffed banana slices. Various image-based parameters, both in two and three dimensions were assessed and used to monitor the puffing.

Keywords: *Deformation; Puffing; Imge analysis; Physical properties; Surface texture*

1. Introduction

Snacks, especially those made from fruits and vegetables, have recently received increasing attention and are widely consumed by health-conscious consumers. Such an increased consumption is due to the fact that modern consumers are paying more attention to their health and trying to switch from traditional to non-sugary and low-fat or even fat-free snacks. Low-fat or fat-free snacks, which are produced by hot air drying, however, suffer important drawbacks; these snacks generally exhibit inferior texture to those obtained via the process of frying. An alternative drying technology is clearly needed to alleviate the drawbacks. Combined hot-air and microwave drying has indeed been suggested and applied to produce dried fruit snacks with more desirable texture.[1] The superior texture is due to puffing, which occurs due to rapid expansion of the fruit microstructure as a result of rapid internal evaporation of water into vapor that cannot escape from such a microstructure at an adequate rate.

Puffing is generally evaluated and reported in terms of volumetric deformation, which is calculated as the ratio of the volume of a sample after drying to that before drying.[2] However, volumetric deformation cannot be used to describe non-uniform or irregular puffing, which normally takes place and can significantly affect the appearance and hence the consumer's acceptance of a final product.[3] It has in fact been reported that two pieces of a material may exhibit similar volumetric shrinkage (or deformation) despite the fact that they had gone through different methods of drying and clearly possess different forms (shape and size) of deformation.[4]

Although image analysis has been used in some earlier studies to evaluate deformation during drying, attempts were usually made only to evaluate deformation in one or two dimensions, which is not adequate when a sample deforms non-uniformly[3] or exhibits irregularly rugged surface in three dimensions such as in the case of puffing. This is simply because one and two dimensional imagings are much easier than three-dimensional imaging, eventhough they cannot accurately well represent deformation.[3] In addition, despite some recent attempts to describe deformation using indicators derived from image-based information, most studies only focused on uniform deformation of simple shapes, e.g., spherical, cylindrical and cubical shape.[3] The ability to precisely identify the shape and its changes of an irregularly shaped materials remains a challenge.

In this study, the use of combined hot-air and microwave drying to dry and puff banana slices was first evaluated. Algorithms and software were developed to characterize the changes in the appearance of puffed banana slices. Various image-based parameters, both in two dimensions (i.e., projected area, major and minor axes, equivalent diameter, perimeter, fractal dimension, extents, form factor and aspect ratio) and three dimensions

(i.e., image-based volume, surface area, sphericities, Wadell's roundness, radius ratio and Hoffmann shape entropy), were assessed and used to monitor the puffing.

2. Materials and Methods

2.1. Banana slices preparation

Banana of the Namwa variety (*Musa sapientum* L. (ABB group)) was used in this study. Banana was purchased from a local supermarket and kept at room temperature (28° ± 3° C) until its total soluble solids (TSS) reached 28.5° ± 0.5º Brix. Banana was peeled and sliced to the dimensions of 5 ± 0.5 mm in thickness and 30.0 ± 2.0 mm in diameter; the dimensions were measured by a Vernier caliper (Winston, Japan).

2.2. Drying and puffing experiments

Drying experiments were conducted in a convective hot-air dryer (Memmert, UF30, Germany) at 70° ± 5° C until the banana moisture content reached either 10, 20, 30 or 40% dry basis (d.b.). Puffing was then conducted in a domestic microwave oven (Samsung, MS23K3513AW, Malaysia) at an input powder of 800 W for either 0, 20, 40 or 60 s.

2.3. Image acquisition

Two-dimensional images of banana slices were first taken via the use of a scanner (Epson, V30, Indonesia) at 300 dpi with black background to reduce the shadow. Three-dimensional images were produced from the two-dimensional images as per the procedures developed by Jinorose et al.[3] Two-dimensional images were preprocessed by MeshLab (ISTO-CNR, Visual computing Laboratory) to reduce unwanted objects and then reconstructed using Autodesk Recap 360 software (Autodesk Inc., San Rafael, CA) into three-dimensional images.

2.4. Image aanalysis

Each 2D image was preprocessed and analyzed using MATLAB® (version R2015b, MathWorks Inc., MA). Image segmentation was conducted by converting RGB image into binary image using Otsu's thresholding method. Edge detection and holes filling were performed to segment the area of interest (AOI). All the basic image parameters including projected area, major axis length, minor axis length, equivalent diameter, perimeter and extent were calculated using the functions of MATLAB® image processing tools box. Other parameters were also calculated as per the following equations.[5]

$$\text{Extent 2} = \frac{A}{D_{\text{fmax}} D_{\text{fmin}}} \quad (1)$$

$$\text{Form factor} = \frac{4\pi A}{P^2} \quad (2)$$

$$\text{Aspect ratio} = \frac{D_{\text{fmax}}}{D_{\text{fmin}}} \quad (3)$$

In the case of 3D analysis, after a 3D image was reconstructed, the image was converted into an STL file and imported into COMSOL Multiphysics® version 3.5 (COMSOL, Inc., Sweden) to calculate the image-based volume, surface area, sphericity, Wadell's sphericity, Wadell's roundness, radius ratio and Hoffmann shape entropy.[5,6] 'fine mesh' setting was adopted when assigning meshes to the object prior to the calculation.

$$\text{Sphericity} = \frac{(36\pi)^{\frac{1}{6}} V^{\frac{1}{3}}}{SA^{\frac{1}{2}}} \quad (4)$$

$$\text{Wadell's sphericity} = \frac{SA_{\text{V}}}{SA} \quad (5)$$

$$\text{Wadell's roundness} = \frac{4A}{\pi D_{\text{fmax}}{}^2} \quad (6)$$

$$\text{Radius Ratio} = \frac{R_{\text{min}}}{R_{\text{max}}} \quad (7)$$

$$\text{Hoffmann shape entropy} = \frac{1}{\ln(\frac{1}{3})} \sum_{i=1}^{3} p_i \ln p_i \quad (8)$$

2.5. Moisture content determination

The moisture content of a sample was determined as per AOAC method 984.25 (2000).

2.6. Volume determination

The volume of a sample was determined as per the methods of Yan et al.[7] The sample was suspended in 125 mL of 95% *n*-heptane, which was filled in a 250-mL beaker placed on a 3-digit balance (Want, WT3203N, China).

All experiments were performed in triplicate and the results, where appropriate, are reported as mean values and standard deviations.

3. Results and discussion

3.1. Drying of banana slices

Preliminary experiments revealed that banana slices suffered phase transition and stuck to the tray when drying was conducted at 90° C. Drying was therefore conducted at 50 and 70° C; the degrees of puffing (or deformation) and visual appearance were noted to be almost the same at the same moisture content either when drying was conducted at 50 or

70° C. As a result, drying at 70° C was finally selected in the interest of time and energy conservation.

3.2. Puffing of banana slices

After drying to the predetermined moisture content, puffing was conducted. Selected images of the samples at different puffing time are shown in Fig. 1. Deformation occurred rather uniformly until about 40 s, after which the sample started to deformed non-uniformly. This visually observed critical point corresponded to the moisture ratio of around 0.4-0.5 (Fig. 2a).

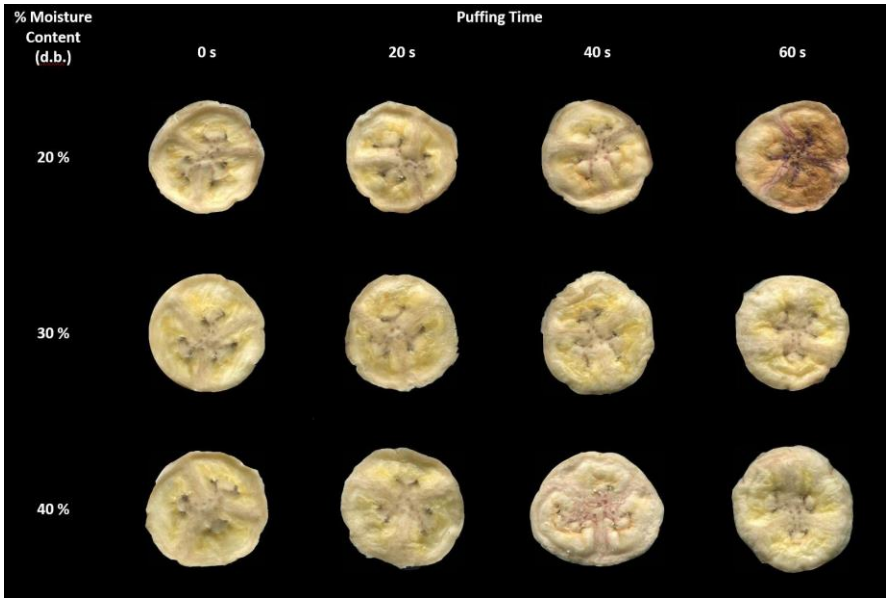

Fig. 1 2D images of banana slices during puffing.

The evolution of the degree of puffing (volumetric deformation) as a function of the moisture ratio with moisture content prior to puffing as a parameter is shown in Fig. 2b. Degree of puffing increased linearly even when the moisture ratio reached around 0.2 (or the puffing time of around 60 s as seen in Fig. 2a). It is important to note that the degree of puffing, which was obtained from liquid displacement measurement, could not identify the start of the non-uniform deformation period, which took place at around 40 s as mentioned earlier.

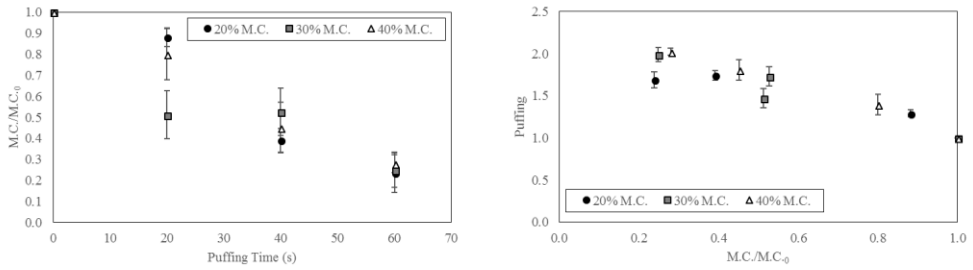

(a) (b)

Fig. 2 (a) Moisture ratio as a function of puffing time of banana slices. (b) Degree of puffing of banana slices as a function of moisture ratio.

3.3. Image-based information

Fig. 3a shows the evolutions of the 2D image-based parameters as a function of the moisture ratio of banana slices undergoing puffing. When considering which parameters could be used to describe the non-uniform deformation (or, in other words, change of shape), only the aspect ratio and extent 2 could be used. It is seen that while other parameters stayed unchanged, these two parameters started to vary significantly when the moisture ratio was around 0.5, beyond which their values started to increase. This corresponded to the critical point where non-uniform deformation was observed to start (see Fig. 1). Nevertheless, these two parameters could only identify the onset of the non-uniform deformation but not the deformation itself. These 2D parameters could also not be used to monitor the volume change of the samples, as expected. Since puffing naturally involves the change of volume, inability to monitor such a change is clearly inadequate.

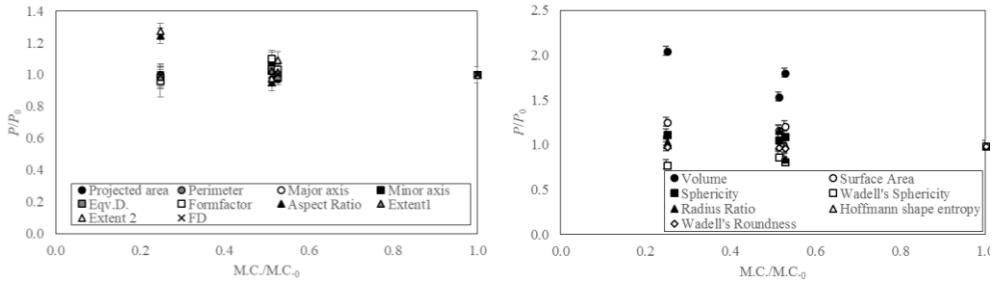

(a) 2D image-based parameters (b) 3D image-based parameters

Fig. 3 (a) Evolutions of image-based parameters as a function of moisture ratio of banana slices undergoing puffing. P = parameter of interest; 0 = initial value.

Interestingly, form factor and fractal dimension, which are widely used to indicate circularity and shape changes, remained unchanged over the whole puffing period. This incorrectly implies that banana slices retained their shape throughout the process, which contradicted to the visual observation results. This is most probably because 2D top-view images are not adequate for the evaluation of a sample with rugged surface (as in our case of puffed banana slices). For this reason, choosing appropriate parameters is very important if non-uniform deformation is to be monitored; widely used parameters cannot always be used for such a purpose.

Fig. 3b shows the evolutions of the 3D image-based parameters as a function of the moisture ratio of banana slices undergoing puffing. The volume and surface area values were those of the reconstructed 3D images; the values increased with decreasing moisture ratio. Only the Wadell's sphericity exhibited a similar trend to the aspect ratio and extent 2 (started to decrease after the moisture ratio was lower than 0.5) and might be able to be used to monitor the non-uniform deformation.

Based on the aforementioned observations, volume and surface area along with the Wadell's sphericity should be used to monitor the puffing of banana slices. Fig. 4 indeed illustrates that the volume as obtained from image analysis agreed well with the values obtained from the liquid displacement experiments.

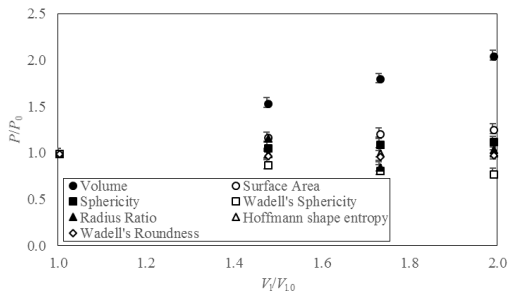

Fig. 4 Evolutions of 3D image-based parameters as a function of volume ratio of banana slices undergoing puffing. P = Parameter of interest; 0 = initial value.

4. Conclusions

Image analysis algorithms were developed to characterize puffing, which is a non-uniform deformation phenomenon, of banana slices in three dimensions. Various image-based parameters, both in 2D and 3D, were calculated and tested for their suitability to monitor such a deformation. As for the 2D-based parameters, aspect ratio and extent 2 could be used to indicate the start of the non-uniform deformation period; Wadell's sphericity represented the 3D-based parameters that could be used to perform the similar task. These parameters, however, could not be used to monitor the volume change of the samples. 3D-based volume

and surface area along with the Wadell's sphericity should instead be used to monitor the puffing of banana slices.

5. Acknowledgements

The authors express their sincere appreciation to the Thailand Research Fund (TRF) for supporting the study financially through its New Researcher Grant awarded to Author Jinorose (Grant No. TRG 5880109) and Senior Research Scholar Grant awarded to Author Devahastin (Grant No. RTA 5880009).

6. Nomenclature

A	Projected area	cm^2
D_{fmax} , D_{fmin}	Maximum and minimum ferret diameter	m
Major, Minor	Major and minor axis length	cm
P	Perimeter	cm
p_i	Ratio between length of each dimension to sum of length of all dimension in 3D image	
R_{max}	Radius of the smallest circumscribe in 3D image	voxel
R_{min}	Radius of the biggest inscribe sphere in 3D image	
SA	Surface area of sample from 3D image	cm^2
SA_v	Surface area of sphere that have same volume from 3D image	cm^2
V	Volume of sample from 3D image	cm^3

7. References

[1] Paengkanya, S.; Soponronnarit, S.; Nathakaranakule, A. Application of microwaves for drying of durian chips. Food and Bioproducts Processing 2015, 96, 1-11.

[2] Tabtiang, S.; Prachayawarakon S.; Soponronnarit, S. Effects of osmotic treatment and superheated steam puffing temperature on drying characteristics and texture properties of banana slices. Drying Technology 2012, 30(1), 20-28.

[3] Jinorose, M.; Stienkijumpai, A.; Devahastin, S. Use of digital image analysis as a monitoring tool for non-uniform deformation of shrinkable materials during drying. Journal of Chemical Engineering of Japan 2017, 50(1), 785-791.

[4] Devahastin, S.; Niamnuy, C. Modelling quality changes of fruits and vegetables during drying: a review. International Journal of Food Science and Technology 2010, 45, 1755-1767.

[5] Neal, F.B.; Russ, C.J. Measuring Shapes; CRC Press: Boca Raton, 2012; 231-290.

[6] Bullard, J.W.; Garboczi, E.J. Defining shape measures for 3D star-shaped particles: sphericity, roundness, and dimensions. Powder Technology 2013, 249, 241-252.

[7] Yan, Z.; Sousa-Gallagher, M.J.; Oliveira, F.A.R. Shrinkage and porosity of banana, pineapple and mango slices during. Journal of Food Engineering 2008, 84(3), 430-440.

20th International Drying Symposium IDS2016

August 7-10, 2016, Gifu, Japan

Best Research Award

In recognition of excellence in drying research.

Awarded to :

Anyanun STIENKIJUMPAI, Maturada JINOROSE and

Sakamon DEVAHASTIN

板谷義紀

Professor Yoshinori Itaya
Gifu University, Japan
IDS 2016 Chairman

IDS 2016 Gifu

山本修一

Professor Shuichi Yamamoto
Yamaguchi University, Japan
IDS2016 Awards Committee Chairman